KERNFORSCHUNGSZENTRUM

KARLSRUHE

Oktober 1967

KFK 627
SM 101/11
EUR 3671 e

Institut für Angewandte Reaktorphysik
Institut für Neutronenphysik und Reaktortechnik

Physics Investigations of a 670 l Steam Cooled Fast Reactor System in SNEAK, Assembly 3A-1

L. Barleon, A. Bayer, R. Böhme, K. Böhnel, K. Burkart, J.C. Chou, P. Engelmann, G. Fieg, F.W.A. Habermann, D. Kuhn, W. Mayer, M. Metzenroth, A. Raberain, H. Seufert, D. Stegemann, P.L. van Velze, H. Walze, H. Werle, D. Wintzer

GESELLSCHAFT FÜR KERNFORSCHUNG M.B.H.

KARLSRUHE

KERNFORSCHUNGSZENTRUM KARLSRUHE

Oktober 1967

KFK 627
SM 101/11
EUR 3671 e

Institut für Angewandte Reaktorphysik
Institut für Neutronenphysik und Reaktortechnik

PHYSICS INVESTIGATIONS OF A 670 ℓ STEAM COOLED FAST REACTOR SYSTEM IN SNEAK, ASSEMBLY 3A-1 *)

L.Barleon, A.Bayer, R.Böhme, K.Böhnel, K.Burkart, J.C.Chou, P.Engelmann, G.Fieg, F.W.A.Habermann[1], D.Kuhn, W.Mayer[2], M.Metzenroth, A.Raberain[1], H.Seufert, D.Stegemann, P.L. van Velze[1], H.Walze, H.Werle, D.Wintzer

(Presented by D.Stegemann)

*) Work performed within the association in the field of fast reactors between the European Atomic Energy Community and Gesellschaft für Kernforschung m.b.H., Karlsruhe.

1) EURATOM Delegate.

2) On leave from Allgemeine Elektricitäts-Gesellschaft, Frankfurt.

Gesellschaft für Kernforschung m.b.H., Karlsruhe

INTERNATIONAL ATOMIC ENERGY AGENCY

SYMPOSIUM ON FAST REACTOR PHYSICS
AND RELATED SAFETY PROBLEMS

October 30 - November 3, 1967
Kernforschungszentrum Karlsruhe, Germany

SM 101/11

PHYSICS INVESTIGATIONS OF A 670 ℓ STEAM COOLED FAST REACTOR SYSTEM IN SNEAK, ASSEMBLY 3A-1 +)

L.Barleon, A.Bayer, R.Böhme, K.Böhnel, K.Burkart, J.C.Chou, P.Engelmann, G.Fieg, F.W.A.Habermann[1)], D.Kuhn, W.Mayer[2)], M.Metzenroth, A.Raberain[1)], H.Seufert, D.Stegemann, P.L. van Velze[1)], H.Walze, H.Werle, D.Wintzer

(Presented by D.Stegemann)

ABSTRACT

A series of experiments is under way at the Karlsruhe Fast Zero Power Reactor SNEAK for the investigation of steam cooled fast reactors in the 100 MWe range. This series started in May 1967 with the critical experiment of SNEAK 3A-1, a 670 ℓ uranium system containing 7.41 x 10^{20} atoms/cm^3 of hydrogen in the form of polyethylene foils. The neutron physics of this assembly has been studied in detail. The neutron energy spectrum has been measured by various methods from the eV-region to over 1 MeV in the core center and at the periphery, reaction rates have been measured in the center and in axial and radial traverses, the initial breeding ratio and the reactivity worth of selected materials have been determined. Measurements of the Doppler reactivity effect, the steam void effect and of ß/l have been performed. Special effort was devoted to the experimental investigation of heterogeneity effects. The experimental results are compared with calculations using the 26 group ABN set and a specially prepared 26 group cross section set KFK-SNEAK using latest cross section information and the SNEAK-3A spectrum as a weighting spectrum. The heterogeneity results are compared with theoretical models including space dependent resonance self-shielding.

+) Work performed within the association in the field of fast reactors between the European Atomic Energy Community and Gesellschaft für Kernforschung m.b.H., Karlsruhe.

1) EURATOM Delegate.

2) On leave from Allgemeine Elektricitäts-Gesellschaft, Frankfurt.

The series of SNEAK-3 experiments is now being continued with the uranium assembly 3A-2 having about twice the hydrogen concentration of 3A-1. After completion of measurements in this system the inner part of the core will be replaced by an equivalent plutonium fuelled zone thus forming the two-zone core SNEAK-3B.

1. INTRODUCTION

For the fast breeder development program a number of considerations - discussed more fully in Ref. [1] - led to the decision to construct one sodium and one steam cooled fast breeder prototype of about 300 MWe in Germany. As a result of this the reactor physics investigations carried out with the fast zero power facilities at Karlsruhe concentrated on assemblies containing hydrogen, because very little information is available about such systems in contrast to those containing sodium. The first exploratory experiments in this line were carried out in STARK [2] and SUAK [3]; now a series of systematic experiments is under way at SNEAK.

Assembly 3A-1 is a 667.2 ℓ uranium fuelled system. The average hydrogen concentration of 7.41×10^{20} atoms/cm^3 corresponds to a steam density of 0.0317 g H_2O/cm^3 in the coolant volume (35%) of a steam cooled fast breeder reactor. The steam is simulated here by polyethylene foils.

Assembly 3A-2 has about twice the hydrogen concentration of 3A-1 so that the corresponding steam density is close to the design value for normal operating conditions in steam cooled fast reactor power plants envisaged at the moment. The experiments in assembly 3A-2 have been started.

The assembly 3B series will follow after completion of 3A-2. The inner part of the core will be replaced by an equivalent plutonium fuelled zone thus forming a two-zone system.

This paper describes the main results obtained in assembly 3A-1. For the evaluation a number of different aspects had to be taken into account:

(a) Comparison of experiment and theory regarding the influence of basic nuclear data together with the weighting spectrum on the preparation of group cross section sets. In this respect comparison has been made to the recently prepared SNEAK set described in Ref. [4] as well as

to the Russian cross section set /5/, referred to as the ABN set. Of primary importance to this aspect are the neutron spectrum, the initial breeding ratio, and the steam void effect.

(b) Comparison of experiment and theory concerning theoretical approximations and numerical procedures which may not be appropriate to systems containing hydrogen. For this purpose different types of calculations have been primarily compared to measured reaction rate distributions in core and blanket in view of power density calculations in steam cooled fast power breeders.

(c) Comparison of experiment and theory referring to heterogeneity effects due to the plate structure in SNEAK in order to derive correction factors for k_{eff} and other quantities of interest. Integral reactivity effects as well as flux fine structure have been measured and compared to a theoretical model including space dependent resonance self-shielding, described in Ref./6/.

The experiments on assembly 3A-1 started in May 1967 and were completed in the middle of September 1967. Taking this into consideration and paying regard to the novelty of hydrogen containing fast reactor systems it can be understood that from the results obtained a number of questions remained open for further investigation.

2. CALCULATIONAL METHODS AND CROSS SECTION SETS USED

The codes for the calculations are part of the Karlsruhe nuclear code system NUSYS and were run on an IBM 7074 computer. For comparison with the experiments of assembly 3A-1 the following codes have been used so far: A one-dimensional diffusion code for cylinder and plate geometry, a one-dimensional S_N code, and appropriate evaluation codes. The number of energy groups was 26 in these cases. The group structure is given in Ref./8/. Furthermore, a two-dimensional diffusion code (DIXY) was applied with 10 energy groups and 1600 space points for the geometry of 3A-1 as shown in Fig.1. The heterogeneity calculations were performed with the code ZERA, described in Ref./6/.

Different cross section sets were used for comparison with measurements and intercomparison of calculations. The three sets are:

(a) KFK-SNEAK set, referred to as SNEAK set. The preparation of the set, the microscopic cross sections used for it, and results of calculations are described in detail in Ref. [4]. Special features of the set are the use of the SNEAK assembly 3A-2 spectrum as a weighting spectrum and the adoption of recently recommended microscopic cross section data.

(b) KFK 26-10 set, referred to as KFK set. This set uses a sodium cooled breeder spectrum as weighting spectrum and was especially prepared for the calculation of such reactors. A description is given in Ref. [7]. Although this cross section set is not particularly suited for the computation of steam cooled fast reactor systems it has, nevertheless, been sometimes included into the intercomparison in order to see trends.

(c) Russian cross section set, referred to as ABN set. A description of the set preparation, together with the data, is given in Ref. [8]. A 1/E spectrum is used as weighting spectrum. An intercomparison of this set was of special interest because it had been used for a series of design calculations.

3. COMPOSITION, CRITICAL MASS AND EFFECTIVE MULTIPLICATION FACTOR

A description of the SNEAK facility and its special experimental equipment is given in Ref. [9]. The actual configuration of assembly 3A-1 is shown in the upper part of Fig.1. In the lower part the idealized dimensions are given, which were the basis for all calculations.

The special platelets and cell structures used in 3A-1 are shown in Fig.2. The steam was simulated by square polyethylene foils of 0.2 mm thickness fixed to stainless steel platelets as indicated. Uranium platelets with 20% (wt) ^{235}U were filled into elements of type 1. Type 2 was composed of those with 35% (wt) ^{235}U together with natural uranium platelets in order to approximate the same average composition in both types. Type 1 dominates in core zone 1 and type 2 in core zone 2. The cell structure for the heterogeneity experiments (see Section 5) is also indicated.

The average atom densities in the different zones are listed in TABLE I. These densities were used for all homogeneous calculations. For the heterogeneity calculations the atom densities are given in TABLE II.

They were calculated by smearing the atom numbers of the platelet together with those of the adjacent stainless steel tube over an area of 29.59 cm^2 (54.4 x 54.4 mm^2). The four platelets in TABLE II form one unit cell for which the atom densities are also given. They are not identical with those used for the homogeneous calculations.

The measured critical mass of the cylindrical reactor with the dimensions shown in Fig.1 is given by:

$$M_{3A-1} = 524.5 \pm 1.0 \text{ kg } ^{235}U$$

This value has been obtained after correcting for the irregular core periphery in the same manner as explained for assembly 1 in Ref./10/. The error arises mainly from the uncertainty in the knowledge of the uranium isotopic composition.

Results for k_{eff} from homogeneous two-dimensional diffusion calculations are given below, together with corrections due to transport and heterogeneity effects:

	SNEAK set				KFK set	ABN set
	Homog.	S_4 correction	Heterogen. correction	Total	Homog.	Homog.
$k_{eff\ 3A-1}$	0.9895	+0.0027	+0.0025	0.995	1.015	1.019

From this comparison it follows that the SNEAK set gives the best agreement with the experiment. Applying equivalent corrections to the KFK and ABN set they underestimate the critical mass appreciably.

4. INVESTIGATION OF THE ASSEMBLY WITH STANDARD CELL STRUCTURE

All experiments described in this section have been performed with a cell structure designated as "normal loading" in Fig.2.

4.1. Neutron spectrum

An intercomparison of calculated neutron spectra at the center of the assembly has been made for the three cross section sets used in order to see their influence on the spectrum. The results are shown in Fig.3.

The spectrum calculated with the SNEAK set has been used as a reference spectrum. Due to the logarithmic scale in the upper part of Fig.3 differences cannot be clearly recognized. Therefore, the ratio of calculated fluxes versus energy is shown in the lower part. Compared to the SNEAK set the spectrum calculated by the KFK set has more flux in group 1 to 7 except group 6. The large discrepancies between both sets in groups 12 to 14 are due to the sodium breeder weighting spectrum. Compared to the spectrum calculated by the ABN set, the SNEAK set produces systematically lower fluxes down to 200 keV and higher fluxes below this value so that the spectrum is remarkably "softened". The same comparison has been made between the three sets for spectra at the core boundary, where the same results were found. Furthermore, spectra calculated at the center and boundary by S_4 approximation were identical to those resulting from diffusion theory.

Spectrum measurements have been performed using the proton recoil spectrometry technique and the ^6Li sandwich spectrometer. Both methods have been applied for measurements close to the core center (position x=19, y=20) for which the results are shown in Fig.4. The proton recoil measurements were made with spherical proportional counters. Gas type (H_2 and CH_4), gas pressure, and high voltage were adjusted to the energy range of interest. For the low energy part a γ-discrimination technique, described in Ref. [11,12], was applied. The proton recoil data were corrected for wall effects. The ^6Li semiconductor sandwich spectrometer was used to measure the high energy part of the spectrum. The ^6Li foil between the detectors could be removed for background measurements and had a thickness of 57 $\mu g/cm^2$ ^6LiF. The pulse height distribution was unfolded using measured response functions in order to derive the neutron spectrum. The ^6Li data were fitted to the proton recoil data around 1 MeV. Full details of both spectrometry techniques, including the performance of analysis, are given in Ref. [13]. Measurements with the proton recoil counters have also been made at the core boundary (position x=19, y=28). The results are shown in Fig.5.

A comparison of measured and calculated neutron spectra in both positions is shown in the lower part of Fig.4 and 5, respectively. Because the neutron spectrum is strongly space dependent at the core boundary a special zone according to the dimensions of the counter was introduced into the calculations so that an average neutron spectrum of this zone was available to compare with the measurements. The measured data were

averaged over corresponding energy groups. Those parts of the measured and calculated spectra to be compared were normalized to equal area and the ratio of equivalent ϕ_i was formed. Although we are aware of the fact that the structure of 26 energy groups is much too coarse for a detailed analysis, the comparison allows, nevertheless, certain conclusions. For both positions the calculated spectrum using the SNEAK set gives from group 5 to 10 (approximately half width of $\phi(u)$ maximum) much better agreement with the experiment than the ABN set. Common to both positions and sets is that a broader distribution of $\phi(u)$ seems to be calculated than measured.

To gain knowledge about the neutron spectrum below 5 keV resonance activation foils in sandwich geometry have been irradiated at the center of the assembly. A description of this method is given in Ref. [14]. Data from the foils used for this experiment are given in TABLE III. The foil diameter was 18 mm. They were covered by Cd of 0.5 mm thickness and positioned in a cavity at the core center. Only foils of the same material were irradiated at the same time. The neutron flux level was monitored for each irradiation.

The results of the sandwich experiments are shown in Fig.6. They have been plotted together with the other experimental data and the calculated spectrum (SNEAK set). The ^{23}Na results were used to normalize experiment and calculation. Error margins have not been given because no detailed information is available so far concerning how the results are affected by either the contribution of higher resonances or the inaccuracy of presently available resonance data. These systematic errors, however, cannot be solely responsible for the fairly large discrepancies between experiment and calculation. The conclusion is, therefore, that the sandwich experiments indicate higher fluxes in the energy range below 200 eV compared to calculation with the SNEAK set.

4.2. Spectral indices

Measured and calculated spectral indices at the center of the assembly are given in TABLE 4. Indices No.1 to 4 were measured by absolutely calibrated parallel plate fission chambers positioned in a cavity at the center of the core. Index No.5 was measured by irradiating uranium foils (0.2 and 19.8 % ^{235}U) attached to a parallel plate fission

chamber containing ^{235}U. During the irradiation time the pulses from the fission chamber were counted so that the foil was calibrated against the fission chamber. The ^{238}U capture rate was determined absolutely by the technique described in Ref. /15/. Indices 6 to 8 were also measured by foil activation. The ^{235}U fissions were determined again via the calibrated ^{235}U fission chamber and the activity of the other foils was determined by absolute counting techniques. All the experiments were monitored by three intercalibrated monitor channels in order to cover the whole power range of interest. They were used as reference points so that the different experimental runs could be compared and cross-checked.

The comparison between experiment and calculation regarding indices No.1 to 3 shows the largest deviations from the experiment for the calculations performed with the SNEAK set. This fact is not understood yet and will be further investigated. This includes a recalibration of the parallel plate fission chambers and an improvement of fission foil fabrication, which is under way now. For index No.5 the agreement is best for the SNEAK set. This is of special interest in connection with the initial breeding ratio determination discussed further below. Index No.6 shows less ^{23}Na captures than calculated by the SNEAK set.

4.3. Fission and capture rate traverses, initial breeding ratio

Radial and axial traverses of ^{235}U and ^{238}U fission rates and ^{238}U capture rates have been measured along one radius and along the central axis of the reactor. For the determination of fission rates two different experimental techniques were applied. In the one case a stack of four small cylindrical fission chambers (20^{th} Century Electronics, G.B., Type FC4) were placed in a 17 x 17 mm^2 guide tube within an element at position x=19, y=18. The remaining volume of the element was filled with platelets of smaller size in a way that the average core composition was closely approximated. These chambers with different layers served to map the axial fission rate distribution. The same stack was positioned in the horizontal drawer, designated by H in Fig.1, to measure the radial distribution. In the other case uranium foils were inserted into the standard cell where Al_2O_3 platelets were replaced by aluminium foil holders in order to measure the axial traverse. For the radial traverse the foils were inserted into the pockets of the horizontal drawer, which had a somewhat different cell pattern. Two uranium foils (0.2 % and 20% enriched)

separated by an aluminium foil were placed into one foil holder so that ^{235}U fissions, ^{238}U fissions, and ^{238}U captures could be determined from one irradiation.

The results of both types of fission rate measurements agreed within 1 to 2% over the core volume, whereas discrepancies up to 10% were observed for points measured in the outer blanket. The foils gave systematically higher values than the chambers. This may be partly due to streaming effects caused by the guide tube of the chambers and, perhaps, partly due to the presence of enriched foils in the depleted blanket material. This discrepancy will be studied in more detail. The experimental results for radial and axial ^{235}U fission rate traverses, obtained with chambers, are shown in the upper part of Fig.7. The corresponding results for ^{238}U fission rates, also from chambers, are plotted in Fig.8. ^{238}U capture rate traverses in axial and radial directions measured by foils are shown in Fig.9.

Reaction rates have been calculated in three different ways:

(a) Calculation by a one-dimensional diffusion code in plate and cylinder geometry for which the radial and axial bucklings were properly chosen to render the reactor critical.

(b) Calculation by a one-dimensional S_4 code in the same manner as in (a).

(c) Calculation by a two-dimensional diffusion code with the reactor dimensions given in Fig.1 and the composition given in TABLE I.

The shapes of the reaction rate traverses from these calculations were intercompared and were found to be almost identical.

Comparison of experiment to these calculations has been made by plotting the ratio of calculated to measured reaction rates as function of radius and core height in the lower part of the corresponding figure. In general, there is fairly good agreement within the core except towards the boundary, but there is strong disagreement in the blanket regardless of the cross section set used. The strong discrepancy in the blanket region is believed to be mainly due to the theoretical treatment of resonance self-shielding in the different reactor zones. In the codes used the self-shielding factors are calculated for one complete zone according to composition. These factors change, therefore, stepwise by crossing the zone boundary. The strong space dependence of resonance self-shielding between

zones of different composition is not taken into account. It is apparent that discrepancies between experiment and theory due to this treatment become more visible the more the number of neutrons in the resonance region is increased by softer spectra.

Reaction rate ratios could also be derived from the measurements, because the cylindrical fission chambers were calibrated against the parallel plate fission chambers, and the ^{238}U capture rate was measured absolutely by the procedure described in Ref. [15] and was also corrected for heterogeneity effects. The results are shown in Fig.10. The ratios plotted are the quotients of the reaction rates per atom. Comparison of calculation and experiment is made by forming the quotient of calculated to measured reaction rate ratios.

The initial breeding ratio (IBR), defined in this case as

$$IBR = \frac{^{239}Pu \text{ produced by capture in } ^{238}U}{^{235}U \text{ consumed by fission and capture}}$$

has also been investigated. For this purpose the integral fission and capture rates INT ^{235}U fission, INT ^{235}U capture, and INT ^{238}U capture were determined by integrating over core and blanket. The initial breeding ratio follows as:

$$IBR = \frac{\text{INT } ^{238}U \text{ capture}}{\text{INT } ^{235}U \text{ fission} + \text{INT } ^{235}U \text{ capture}}$$

The theoretical IBR was derived from two-dimensional diffusion calculations with the actual geometry and composition of the assembly. The results are given in TABLE V. Comparing the theoretical values it has to be kept in mind that the calculated reactors were not exactly critical as discussed in Section 3. From the experiment, INT ^{235}U fission and INT ^{238}U capture have also been determined by integration, taking into account the actual composition in the different zones. Because the experimental data agreed best with the theoretical results using the SNEAK set the corresponding reactor averaged ^{235}U capture to fission ratio has been used to derive the "experimental" IBR given in TABLE V. The error margins indicated result from a fairly rough error estimation due to the fact that only one radial and one axial traverse for each reaction rate was used for the evaluation.

4.4. Prompt neutron decay constant

Prompt neutron decay constants have been measured by the pulsed source technique. A 150 kV Cockroft-Walton type accelerator with duoplasmatron ion source, designed by W.EYRICH, was used. Characteristic data of the neutron generator are: pulse width about 1 /usec, repetition frequency up to 2000 pulses per sec, maximum source strength about 5×10^4 neutrons per pulse. The target was positioned within the open half of the horizontal channel close to the core center. A ^{235}U fission chamber was located at position x=22, y=18. As time analyzer a fast 32 channel shift register (manufactured by BORER and Co., Solothurn, Switzerland) with scaler memory was used, as described in Ref. /16/.

Prompt neutron decay constants were measured at several subcritical states from about 2 dollars to a few cents below delayed critical. The experimental value for the prompt neutron decay constant α_c, obtained by extrapolation to delayed critical, is given in TABLE VI, together with calculated values using $\beta_{eff} = 7.1 \times 10^{-3}$.

The comparison of the data shows the well known overestimation of α_c by calculation. The SNEAK set gives a value closest to the experimental one.

4.5. Material worth measurements

A number of sample reactivity measurements were made using the horizontal drawer and the sample changer (see Ref. /9/). Except for the sample position the drawer was filled with core material in order to minimize perturbation of the core.

Two series of measurements have been performed. In the first series the samples were contained in otherwise empty stainless steel boxes of 2 x 2 x 1 inches. Central reactivities of these samples were measured by the asymptotic period technique. A period measurement with a reference box was made before the various samples were measured at the core center. It was not necessary to interrupt reactor operation since the resulting reactivity variations were made small enough to prevent large power fluctuations. The reactor periods were generally larger than 1000 sec; flux data were collected during 10 min for each sample.

In the second series of measurements the remaining space in the box was filled with core material. Those boxes were used for radial reactivity traverses with some of the samples, for which the central worths had

been measured. The inverse kinetics method was used to determine reactivities during the traverses. The sample was stopped for 5 min at each position in order to reduce the effect of removal of delayed neutron precursors from the reactor, caused by the movement of core material in the sample drawer. This period was also long enough to collect sufficient flux information for a statistically accurate reactivity calculation.

The material worths have been calculated against void by a perturbation calculation in which a very small quantity (generally 10^{20} atoms) of the perturbing sample material was added to 1 cm^3 of core mixture. The dimensions and the transverse buckling correspond to the actual dimensions of the critical reactor.

Measured and calculated central reactivity worths are compared in TABLE VII. Measured and calculated radial reactivity traverses are shown in Fig.11. The data are not normalized. Poor agreement between calculation and experiment is found especially for graphite, aluminium, and CH_2. The ABN set generally gives values closer to the experiment except for ^{239}Pu and Cr. In order to start investigations to resolve the discrepancies between theory and experiment the influence of the surroundings has been studied. The comparison of the two experimental procedures I and II shows that these effects are small compared to the discrepancies.

4.6. Reactivity worth of control rods

Assembly 3A-1 contains ten shim rods, six safety rods, and one fine control rod as shown in Fig.1. All rods are filled with core material in such a way that the reactor has a homogeneous core composition with all rods inserted. The shim rods have poison followers of B_4C powder, the safety rods have followers of a solid dispersion of this powder in epoxy resin. The followers protrude axially through the largest part of the core with the rods in the shutdown position.

The ten shim rods and two of the safety rods were calibrated by the continuous run method. The fine control rod and two of the shim rods were also calibrated by moving the rod stepwise in order to obtain better statistics at some rod positions for the reactivity worth as derived with the inverse kinetic equations from the flux history. The neutron flux was detected by two ionization chambers at opposite positions (x=11, y=31) and (x=26, y=06) just outside the blanket, as indicated in Fig.1.

Measured and calculated reactivity worths of shim rods are given in TABLE VIII. It can be seen from the values that the measured rod worth depends on the position of the ionization chamber. The differences are larger than could be expected from statistical uncertainties. The ionization chamber which is closest to a rod gives a higher value. This space dependence could not be eliminated by averaging the current of the two chambers. The subcritical measurements also show space dependent effects. During these measurements an AmBe source was inserted at the core boundary. Its effective strength was determined from the flux history after a reactivity step between two subcritical states. The calibration of the fine control rod was checked with some asymptotic period measurements, the results of which do not depend on the detector location.

The worth of individual shim rods was calculated in the following way: First the central worth of the poison part of a rod as compared to core material was determined by a one-dimensional diffusion calculation (with KFK set) in cylindrical geometry with an axial buckling corresponding to the extrapolated height of assembly 3A-1. The poison part of the control rods does not fill the core over the whole axis; the calculated central poison worth was converted to the worth of a rod in its actual geometry by $\cos^2$ weighting. The worths of rods at the various radial locations were finally obtained from the central one by J_o^2 weighting.

Those calculations were cross-checked by a calculation in (r,θ) geometry for shim rod T1, using the SNEAK set and 6 energy groups. Both values agreed within 5%.

5. INVESTIGATION OF HETEROGENEITY EFFECTS

All experiments and results described in this section have been made by changing the normal cell structures to "bunched" cell structures in parts of the core volume. The two types of bunching, namely single bunching and double bunching, are indicated in Fig.2.

A series of bunching experiments in different core positions has been performed to measure the influence of heterogeneity on k_{eff} and to get some information about the leakage component of heterogeneity effects.

5.1. Integral heterogeneity effects

(a) Radial dependence of bunching effects in the central test zone

A central zone, consisting of 21 fuel elements was bunched (single bunching) in 6 successive steps as indicated in Fig.12a. The numbers 1 to 6 correspond to the number of the step. The resulting reactivity effects per element in cents, together with calculated values, are also shown in Fig.12a. They show that the bunching effects are nearly additive and that the smaller values for the last steps can be explained by a loss of importance with increasing radius. The conclusion is drawn that a zone of 21 bunched elements is large enough to neglect surface effects of the bunched zone.

The calculated values have been obtained by perturbation calculations with "heterogeneity corrected" cross sections. These cross sections are an extract of multigroup cell calculations performed with the code ZERA. Details of the calculation methods are explained in Ref. [6].

(b) Variation of the axial extension of the bunched zone

The axial extension of the bunched region of 21 central elements has been varied in 4 steps: 16, 32, 48, and 64 cells corresponding to 1/4, 1/2, 3/4, and full core height. The experiments have been done to look for heterogeneity effects on global diffusion in a direction perpendicular to the plate surfaces. In Fig.12b the measured reactivity effects are compared to theoretical values. The latter have been calculated without modifications of the diffusion properties. From the agreement it follows that heterogeneity effects on diffusion perpendicular to the plates can be neglected, as is discussed more generally in Ref. [6].

(c) Reactivity effect of double bunching in the central zone

The effect of double bunching the 21 central elements over the full core height has also been measured. The resulting reactivity change is shown in Fig.13a, together with the results of single bunching. Calculated values for single and double bunching as well as for the homogeneous case are also shown. Whereas the calculated result using the SNEAK set agrees fairly well with the experiment, the one using the ABN set shows poor agreement. One reason for this can be found from fine structure measurements and is discussed in Section 5.2.

(d) Reactivity effects of bunching near the core boundary

It was expected that the heterogeneity effects of elements near the core boundary are strongly influenced by a kind of "streaming" effect due to platelets with small transport cross sections. Therefore, the bunching experiments have been continued at the periphery of the core as indicated in Fig.13b. The reactivity changes after bunching of two groups of elements over the full core height with slightly different mean radial positions at the periphery are shown in Fig.13b (right side) for two degrees of bunching ($l/l_1 = 2$ and $l/l_1 = 4$). The effects become negative near the core edge.

The relative differences between experimental and calculated values are larger than in the core center, but the change in sign of the bunching effect is in satisfactory agreement with the calculated curve. The designation theory I means that the calculation has been performed without changing diffusion coefficients, whereas theory II includes heterogeneity corrections to the diffusion coefficients.

To confirm that the negative heterogeneity effects near the core periphery are really due to changes in radial diffusion properties, the two following experiments have been performed:

1. Thirteen elements in the boundary core zone were loaded as shown schematically in Fig.14a. The platelets were vertically positioned over 7/16 of the core height so that their surface normals had a direction nearly parallel to the flux gradient. In this direction streaming channels are avoided. The reactivity effects caused by bunching these vertically positioned platelets are also shown in Fig.14a. They agree rather well with the values calculated without changing the radial diffusion coefficients during bunching.

2. The 13 elements have been turned around in four steps of 90° for each of the three cell structures ($l/l_1 = 1$, 2, and 4) with the platelets vertically positioned. As indicated in Fig.14b in two of the four steps the surface normal of the vertically positioned platelets was either parallel or perpendicular to the flux gradient. The mean reactivity value of the two "parallel" steps was compared to the mean value of the two "perpendicular" steps. The reactivity difference shown in Fig.14b is obviously caused by the difference between the diffusion coefficients parallel and perpendicular to the platelets. Since the heterogeneity influence on the latter is small, it is essentially the influence of heterogeneity on leakage parallel to the platelets which has been measured. An increased leakage and its ne-

gative reactivity contribution is always present for the outer parts of the core if the platelets are horizontally positioned, which is the normal case. This negative contribution, however, is strongly compensated by the positive reactivity contribution due to bunching, found in experiment 1. This is consistent with the results shown in Fig.13b for the boundary core zone.

5.2. Investigation of flux fine structure

The results of fine structure measurements shown in Fig.15 and 16 give some more differential information about the heterogeneity effects. The main contribution to the $^{103}Rh(n,n')Rh^{103m}$ activation and to ^{238}U fission is caused by neutrons with energies above 200 keV and 1 MeV, respectively. A comparison of the measured cell traverses with the results of ZERA calculations show that the flux fine structure for high energy neutrons is in good agreement to the experiment, if the SNEAK set is used. Calculations with the ABN set underestimate the space dependence of the $^{103}Rh(n,n')$ activation strongly. This gives an insight into why the reactivity effects due to bunching, which in this case get their main contribution from the high energy part of the spectrum, are underestimated by the ABN set, as shown in Fig.13a.

The agreement between experiment and calculation (SNEAK set) is not so good for the fine structure of the ^{238}U capture rate shown in Fig.16. The calculations seem to underestimate the space dependence within the uranium platelets. This is to be expected because the spectrum measurements by foils, shown in Fig.6, and lifetime measurements indicate more neutrons in the 10 to 100 eV range than calculated. It is just this region where self-shielding effects are especially large.

Probably the discrepancy between measured and calculated ^{235}U fission rate distributions within the cell, shown in Fig.15, is due to the same reasons. The ^{235}U fission curves result from a partial compensation of a flux depression (within the uranium platelets) at low energies and a flux peaking at high energies. Small errors in the rate distribution caused by low energy neutrons will, therefore, lead to large errors in the resulting ^{235}U fission rate distribution.

Generally, it can be stated that such fine structure measurements are sensitive to changes in the overall neutron spectrum. They can, therefore, be used to test cross section sets, provided that the calculational methods used for fine structure investigations are sufficiently accurate.

5.3. Additional results obtained during the bunching experiments

Pulsed source measurements have been performed when the central zone of 21 elements was doubly bunched. For the prompt neutron decay constant at delayed critical, α_c, no difference could be found within the error limits to that given in Section 4.4. for the normal cell structure. This is in agreement with the heterogeneity calculations performed with the SNEAK set, whereas those with the ABN set predicted a 3% lower value for α_c due to bunching.

Neutron spectrum measurements by the proton recoil technique were also performed in the center of the doubly bunched zone. The resulting neutron spectrum is shown in Fig.17, together with the one obtained for normal cell structure. The position of the spherical counter in respect to the platelets is indicated. A qualitative comparison of the measured spectra shows that the resonances, mainly due to oxygen and aluminium, are less pronounced in the case of double bunching than for the normal cell structure. A quantitative comparison of the two experiments has been made by averaging over groups, normalizing to equal area, and forming the ratio of equivalent fluxes per unit lethargy. This is shown in the lower part of Fig.17, together with the corresponding ratio derived from heterogeneity calculations with the SNEAK set. There are almost no differences for the calculated spectra and only minor differences for the experimental ones, except for the two lowest groups. This, however, should not be overestimated because of the fairly large statistical errors in this region. It can be concluded from this comparison that the overall neutron spectrum above 10 keV is not changed remarkably by double bunching. This is consistent with the result found for the prompt neutron decay constant.

During the phase of single bunching within the central zone temperature dependent reactivity effects of a metallic natural uranium sample were measured using the pneumatic square wave pile oscillator. The construction and the dimensions of the heated sample can be seen from Fig.18. The sample and an equivalent dummy was inserted into a fuel element loaded with core material. The measured reactivity change for temperatures up to 1049°K is shown in Fig.18.

Two types of calculations have been made for this experiment using the method described in Ref. [17], which is part of the NUSYS code system. For the one type the flux depression within the sample was taken into account, whereas this was not the case for the other type. Both calculations were made in cylindrical geometry with diffusion theory. The finite

size of the sample was taken into consideration by a properly chosen σ_p. The calculated results are also shown in Fig.18. The calculation without flux depression yields results approximately 20% higher than the measured values. This shows the influence of flux depression very clearly. The good agreement between experiment and theory for the other case should not be overestimated. In both calculated cases the Doppler coefficient is proportional to $T^{-1.146}$.

6. INVESTIGATION OF THE STEAM VOID EFFECT

The reactivity effect of voiding various core zones in assembly 3A-1 has been measured and compared with calculations.

In a series of experiments the polyethylene foils were removed in a central cylinder of $\bar{r}$ = 14.07 cm, consisting of 21 core elements as indicated in Fig.19. In steps 1a to 1d the polyethylene was removed from the zone in 16, 32, 48, and 64 (full core height) unit cells of each element. This gave the axial dependence of the void effect.

In the following steps 2, 3, and 4 a wider cylinder of 45 elements ($\bar{r}$ = 20.59 cm) and two core sectors have been voided, respectively. From these steps the radial dependence could be derived. The reactivity effect of voiding the total core was extrapolated from the sector experiment. It was assumed that

$$\Delta k_{Void,Core} = \frac{\Delta k_{Void,Sector}}{V_{Sector} / V_{Core}}$$

where $\Delta k_{Void,Sector}$ is the reactivity effect of voiding the second sector. The experimental results for the different steps including the extrapolation to the totally voided core zone are plotted in Fig.19.

Experimental results are compared with calculations in TABLE IX. The experimental error in steps 1 through 4 is mainly due to uncertainties in the worth of control rods used to compensate reactivity. After each step the rods were recalibrated. Deviations in rod worth were in the order of 1% to max. 4% so that the reactivity changes could be determined to about $\pm$ 2%. The reactivity change of voiding the 16 outer elements of step 4 was by 6% smaller than the equivalent one of step 3, indicating that voiding the first sector decreased the flux in this part of the core. The error in the extrapolated value for total core voiding was estimated to be about $\pm$ 7%.

Calculations were made by one-dimensional diffusion codes in cylindrical and plate geometry using transverse bucklings, which rendered the reactor approximately critical in the unvoided case. No two-dimensional calculations have been made so far, nor have final heterogeneity corrections been applied. Preliminary heterogeneity corrections show an increase to the calculated values by a few percent. The experimental values are on the average 16% higher than those calculated with the SNEAK set. Both KFK and ABN sets give a much too small void effect.

7. CONCLUSIONS

Regarding the integral quantities of interest for the design of steam cooled fast reactor systems the agreement between theory and experiment is improved considerably by applying the recently prepared SNEAK set for calculating assembly 3A-1.

The effective multiplication constant, k_{eff}, although underestimated by the SNEAK set is closer to 1 than the fairly strong overestimation by the KFK and ABN set. The underestimation of k_{eff} is decreased to 0.5 % by correcting for transport and heterogeneity effects. The heterogeneity correction in particular is very reliable, as can be concluded from the heterogeneity experiments performed in this assembly. Although the accuracy in k_{eff} is reasonable, further two-dimensional calculations with more than 10 energy groups seem to be interesting in order to see the effect of group collapsing on k_{eff}.

The initial breeding ratio of 1.08 calculated for this assembly using the SNEAK set gives also the best agreement to that derived from the experiment. Concerning the measurements for the determination of the initial breeding ratio it can be concluded that more detailed investigations of reaction rates in the blanket and over the whole core volume are necessary in order to achieve a better experimental accuracy. Measurements within the blanket are particularly important in external breeder systems like this assembly.

The steam void effect experiments also show the best agreement with the results obtained using the SNEAK set. The comparison between experiment and calculation needs to be further extended by the inclusion of two-dimensional calculations and by investigating in more detail the influence of the neutron spectrum below 1 keV on the steam void effect. It is supposed that the underestimation of the calculated void effect is partly due to the underestimation of the calculated neutron flux below about 300 eV as concluded from the sandwich foil experiments.

From the axial and radial fission and capture rate measurements it can be concluded that a special theoretical effort is necessary to eliminate the fairly large discrepancies between calculated and measured reaction rates at the core boundary and within the blanket. The discrepancies are believed to be partly due to the zone-wise treatment of resonance self-shielding, which is apparently not suitable for steam cooled fast reactor systems with softened spectra.

The results of the heterogeneity experiments showed on the one side the applicability of the theoretical model used to calculate reliable correction factors, because the integral reactivity effects of the bunching experiments as well as their trends were very well predicted in general. On the other side, the calculated heterogeneity results - in particular the flux fine structure - are rather sensitive to changes in the cross section sets. In this respect the SNEAK set also gave the best agreement to the experiment.

From the comparison of calculated and measured neutron spectra it can be concluded that the SNEAK set was also closest to the experiment. This is also true for the results found for the prompt neutron decay constant at delayed critical. There is, however, still a remarkable discrepancy left over.

Whereas the application of the SNEAK set improved the agreement between theory and experiment in all cases mentioned before, this is not so for the material worth measurements and for a few spectral indices. This result is not understood so far.

ACKNOWLEDGEMENTS

The authors gratefully acknowledge the continuous support by the operation staff of the SNEAK reactor during the experiment.

We are also indebted to Dr. H. KÜSTERS for many helpful discussions and to E.A. FISCHER and W. SCHWETJE for performing the Doppler effect calculations and special control rod calculations, respectively.

Furthermore, we thank Dr. W. EYRICH and W. KELLER for their help during the pulsed source experiments.

REFERENCES

/1/ HÄFELE,W., "The German Fast Breeder Project", This Conference, Paper SM 101/5.

/2/ BARLEON,L., BAYER,A., BRÜCKNER,Chr., BURKART,K., KUHN,D., KUSSMAUL,G., MEISTER,H., STEGEMANN,D., "Investigations with Assembly 2 of the Fast-Thermal Argonaut-Reactor STARK", KFK 592, June 1967 (in German).

/3/ KÜCHLE,M., MITZEL,F., WATTECAMPS,E., WERLE,H., "Measurements of Neutron Spectra and Decay Constants with the Fast Subcritical Facility SUAK", Proc. of the Int. Conf. on Fast Critical Experiments and Their Analysis, ANL-7320 (1966) 506.

/4/ BACHMANN,H., HUSCHKE,H., KIEFHABER,E., KRIEG,B., KÜSTERS,H., METZENROTH,M., SIEP,I., WAGNER,K., WOLL,D., "The Group Cross Section Set KFK-SNEAK. Preparation and Results.", This Conference, Paper SM 101/12.

/5/ ABAGJAN, L.P., BAZAZJANC, N.O., BONDARENKO, J.J., NIKOLAEV, M.N., "Group Constants of Fast and Intermediate Neutrons for the Calculation of Nuclear Reactors", States Committee for the Use of Atomic Energy in the UdSSR (in Russian).

/6/ WINTZER,D., "Heterogeneity Calculations Including Space Dependent Resonance Self-Shielding", This Conference, Paper SM 101/13.

/7/ KÜSTERS,H., METZENROTH,M., "The Influence of Some Important Group Constants on Integral Fast Reactor Quantities", Proc. of the Conf. on Safety, Fuel, and Core Design in Large Fast Power Reactors, ANL-7120 (1965) 423.

/8/ ABAGJAN, L.P., BAZAZJANC, N.O., BONDARENKO, J.J., NIKOLAEV, M.N., German Translation of Ref./5/, KFK-tr-144.

/9/ ENGELMANN,P., BICKEL,W., DÄUNERT,U., HABERMANN, F.W.A., VAN VELZE, P.L., WALZE,H., WITTEK,G., "Construction and Experimental Equipment of the Karlsruhe Fast Critical Facility, SNEAK", Proc. Int. Conf. on Fast Critical Experiments and Their Analysis, Argonne, ANL-7320 (1966) 725.

/10/ BARLEON,L., BÖHME,R., BÖHNEL,K., EDELMANN,M., ENGELMANN,P., FIEG,G., HABERMANN, F.W.A., KUHN,D., MAYER,W., SEIFRITZ,W., STEGEMANN,D., VAN VELZE, P.L., WALZE, H., WERLE,H., "Comparison of Measurements in SNEAK-1 and ZPR 3-41", This Conference, Paper SM 101/8.

/11/ BENNETT, E.F., "Neutron Spectrum Measurements in a Fast Critical Assembly", Nucl. Sci. Eng. 27 (1967) 16-27.

/12/ STRAUSS, M.G., BRENNER,R., "General Purpose Analog Pulse Height Computer", Rev. Sci. Instr. 36 (1965) 1857.

/13/ BLUHM,H., FIEG,G., LALOVIC,M., STEGEMANN,D., WATTECAMPS,E., WERLE,H., "Fast Reactor Spectrum Investigations on the Facilities SUAK and SNEAK at Karlsruhe", ANS-Transactions, Vol.10, No.2 (1967) (Full text to be published).

/14/ EHRET,G., "The Measurement of Epithermal Neutron Spectra by Use of Resonance Detector Foils (Sandwich Method)", Atompraxis 1 (1961) 393-400.

/15/ SEUFERT,H., STEGEMANN,D., "A Method for Absolute Determination of ^{238}U Capture Rates in Fast Zero-Power Reactors", Nucl. Sci. Eng. 28 (1967) 277-285.

/16/ EDELMANN,M., MURLEY, T.E., STEGEMANN,D., "Investigation of Prompt Neutron Kinetics in the Fast-Thermal Argonaut-Reactor STARK by Noise Analysis, KFK 522 (1967).

/17/ FROELICH,R., "Theorie der Doppler-Koeffizienten schneller Reaktoren unter Berücksichtigung der gegenseitigen Abschirmung der Resonanzen", KFK 367 (1965).

TABLE I Atom densities (in 10^{20} cm^{-3}) of SNEAK 3A-1 used for homogeneous calculations

	Al	C	Cr+Mn	Fe	H	Ni	O	Si	Ti	^{235}U	^{238}U	Mg
Core zone 1	128.8	4.12	36.6	123.1	7.40	19.0	144.7	1.84	0.53	20.314	81.023	0.37
Core zone 2	128.9	4.13	36.7	123.3	7.42	19.0	144.8	1.88	0.55	20.221	81.066	0.37
Blanket zone 3	-	0.14	11.9	40.1	-	10.2	-	0.46	0.2	1.54	399.3	-

TABLE II Atom densities (in 10^{20} cm^{-3}) of SNEAK 3A-1 used for heterogeneity calculations

	Al	C	Cr+Mn	Fe	H	Ni	O	Si	Ti	^{235}U	^{238}U	Mg
SS platelet + CH_2 foil	-	16.01	110.7	373.3	29.48	51.4	-	4.24	1.68	-	-	-
Al platelet (25% Al)	130.1	0.13	12.24	39.54	-	5.86	-	1.30	-	-	-	1.48
U platelet (25% ^{235}U)	-	0.13	11.78	39.54	-	12.9	-	0.44	-	81.282	324.19	-
Al_2O_3 platelet	385.3	0.13	11.78	39.54	-	5.86	578.6	0.44	-	-	-	-
Unit cell	128.9	4.10	36.6	123.0	7.370	19.0	144.6	1.61	0.42	20.320	81.048	0.37

TABLE III Data of resonance activation foils

Isotope	Material	Thickness of foil mm	Lowest resonance energy eV
^{23}Na	NaI crystal	0.5	2850
^{114}Cd	metal	0.5	120.2
^{139}La	metal	0.250	72.4
^{186}Wo	metal	0.025	18.8
^{98}Mo	metal	0.2	12 (467)
^{197}Au	metal	0.025	4.906
^{115}In	In-Pb alloy	0.050	1.456

TABLE IV Spectral indices at the center of assembly 3A-1

No.	Index	Experiment	Calculation			Calcul./Exper.		
			SNEAK set	KFK set	ABN set	SNEAK / Exp.	KFK / Exp.	ABN / Exp.
1	$\frac{^{238}U \text{ fission}}{^{235}U \text{ fission}}$	0.0336 ±5%	0.0301	0.0301	0.0316	0.90	0.90	0.94
2	$\frac{^{233}U \text{ fission}}{^{235}U \text{ fission}}$	1.48 ±3%	1.572	-	1.45	1.06	-	0.98
3	$\frac{^{239}Pu \text{ fission}}{^{235}U \text{ fission}}$	1.03 ±3%	0.958	0.971	1.001	0.93	0.94	0.97
4	$\frac{^{232}Th \text{ fission}}{^{238}U \text{ fission}}$	0.209 ±6%	0.198	-	0.194	0.95	-	0.93
5	$\frac{^{238}U \text{ capture}}{^{235}U \text{ fission}}$	0.142 ±4%	0.143	0.129	0.127	1.01	0.91	0.89
6	$\frac{^{23}Na \text{ capture}}{^{235}U \text{ fission}}$	0.959×10^{-3} ±3%	1.054×10^{-3}	0.846×10^{-3}	0.882×10^{-3}	1.10	0.88	0.92
7	$\frac{^{115}In \text{ capture}}{^{235}U \text{ fission}}$	0.205 ±5%	0.208	-	-	1.01	-	-
8	$\frac{^{103}Rh(n,n')}{^{235}U \text{ fission}}$	0.176 ±10%	0.154	-	-	0.88	-	-

TABLE V Initial breeding ratio (IBR) for assembly 3A-1

	$\frac{\text{INT } ^{238}\text{U capture}}{\text{INT } ^{235}\text{U fission}}$	$\frac{\text{INT } ^{235}\text{U capture}}{\text{INT } ^{235}\text{U fission}}$	IBR
SNEAK set	1.384	0.279	1.081
KFK set	1.307	0.287	1.016
ABN set	1.298	0.298	1.000
Experiment	1.385 $\pm$ 3 %	(0.279)	1.08 $\pm$ 0.03

TABLE VI Prompt neutron decay constant α_c of assembly 3A-1

	Experiment	SNEAK set	KFK set	ABN set
$\alpha_c = \beta/l \left[\text{sec}^{-1}\right]$	$2.05 \cdot 10^4 \pm 2\%$	$2.42 \cdot 10^4$	$2.53 \cdot 10^4$	$2.73 \cdot 10^4$
$\frac{\text{Calculation}}{\text{Experiment}}$	-	1.18	1.23	1.33

TABLE VII Central material worths of SNEAK assembly 3A-1

Material	Sample weight [g]	Sample dimensions [mm]	Measured central reactivity worth [¢/g x 10^3]		Calculation / Experiment		
			I Sample in empty box	II Sample in filled box	SNEAK set / Exper.I	KFK set / Exper.I	ABN set / Exper.I
^{235}U	3.413	46.6x46.6x0.1	+ 33.34 ± 0.6	+ 33.37 ± 0.7	1.15	1.11	1.09
^{238}U	61.56	46.8x46.8x1.6	- 2.41 ± 0.04	- 2.25 ± 0.03	1.20	1.00	0.96
Mo	33.86	46.8x46.8x3.2	- 4.80 ± 0.07	-	1.28	1.23	1.17
C	48.68	46.8x46.8x12.8	+ 5.55 ± 0.1	+ 5.57 ± 0.06	0.25	0.48	0.60
^{10}B	2.90	diam.43x1	-779 ± 1.0	-762 ± 0.7	1.36	1.29	1.16
Al	159.24	50.8x50.8x25.1	- 0.207 ± 0.02	- 0.232 ± 0.02	4.68	3.10	2.05
Ta	53.36	46.8x46.8x1.6	- 14.7 ± 0.08	-	-	-	1.33
SS	108.60	46.8x46.8x6	- 0.97 ± 0.03	- 1.225 ± 0.015	1.37	1.38	1.11
CH_2	2.527	50.8x50.8x1	+234 ± 0.7	+235 ± 0.8	0.66	0.74	0.62
Ni	114.33	46.8x46.8x6	- 1.42 ± 0.06	-	1.73	1.84	1.55
Fe	127.67	46.8x46.8x8	- 0.87 ± 0.05	-	1.47	1.41	1.05
Cr	110.18	46.8x46.8x10	- 0.76 ± 0.03	-	1.39	1.58	1.58
^{239}Pu	28.94	with PuO_2-UO_2	+ 48.1 ± 0.5	+ 50.45 ± 0.5	1.10	1.11	1.12
PuO_2-UO_2	136.45	50x50x5	+ 9.10 ± 0.015	+ 9.71 ± 0.02	1.15	1.15	1.17

TABLE VIII Reactivity worth of control rods in assembly 3A-1

Rod No.	Position (x/y)	Reactivity worth [¢]				
		Inverse kinetic meth.		Subcrit. measurements		Calculation
		Ion chamber 1	Ion chamber 2	Ion chamber 1	Ion chamber 2	(KFK set)
T 1	17/23	102.5	94.0	104.2	102.2	93.1
T 3	23/17	94.8	100.3	94.1	108.1	93.1
T 6	17/14	79.2	82.9	78.5	88.0	75.4
T 8	20/14	84.1	91.1	82.7	97.4	81.2
T 9	14/20	87.1	83.2	86.2	87.7	81.2
T12	23/23	74.3	73.1	78.6	82.3	68.7
T14	26/23	33.1	32.7	-	-	27.3
T15	14/17	78.9	78.8	77.8	82.3	74.9
T16	26/17	43.9	45.4	-	-	40.9
R	11/17	12.35	12.36	12.37 (period measurements)		

TABLE IX Comparison of measured and calculated steam void effects in SNEAK assembly 3A-1

Step	Neg. reactivity effect $\frac{\Delta k}{k}$ [%]				Calculation / Experiment		
	Experiment	Calculation					
		SNEAK set	KFK set	ABN set	SNEAK set	KFK set	ABN set
1a	0.164±0.004	0.130	0.113	0.094	0.79	0.69	0.57
1b	0.304±0.006	0.251	0.217	0.181	0.83	0.71	0.60
1c	0.410±0.008	0.345	0.298	0.248	0.84	0.73	0.60
1d	0.459±0.009	0.386	0.333	0.278	0.84	0.73	0.60
2	0.935±0.018	0.782	0.674	0.563	0.84	0.72	0.60
3	1.079±0.022	-	-	-	-	-	-
4	1.214±0.028	-	-	-	-	-	-
5	3.18 ±0.22	2.67	2.31	1.90	0.84	0.73	0.60

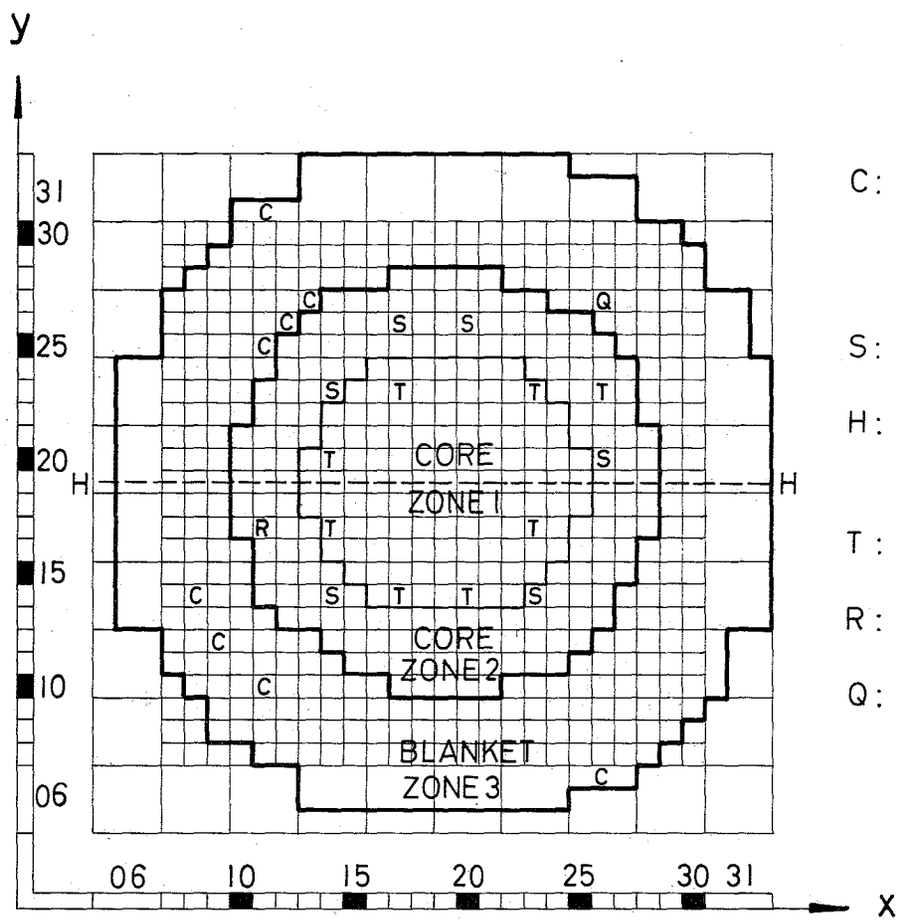

C: ELEMENTS WITH MONITORING DETECTORS

S: SAFETY RODS

H: HORIZONTAL CHANNEL

T: SHIM RODS

R: CONTROL ROD

Q: NEUTRON SOURCE

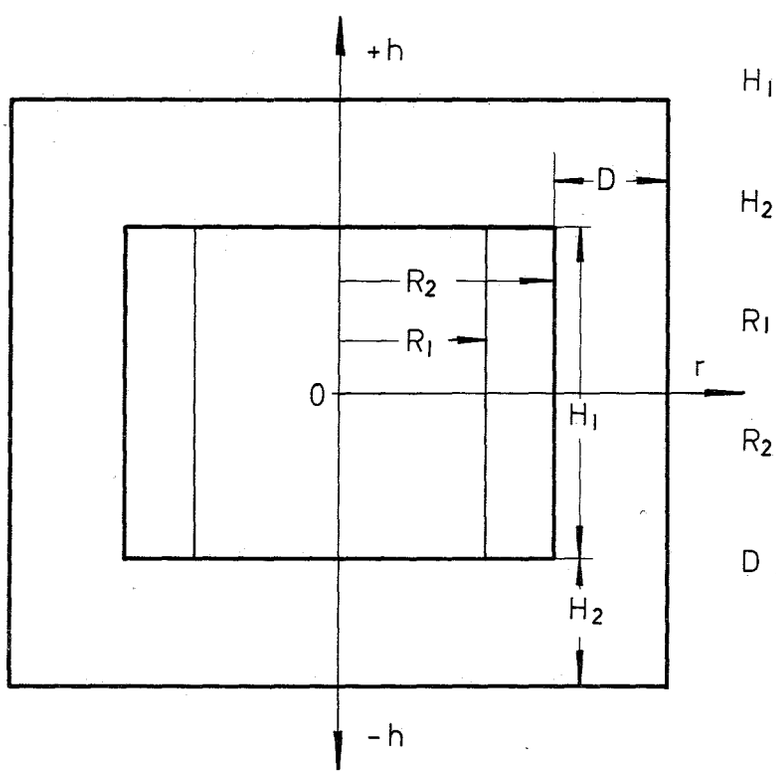

H_1: HEIGHT OF CORE ZONE 80.6 cm

H_2: HEIGHT OF AXIAL BLANKET 30.5 cm

R_1: RADIUS OF CORE ZONE 1 32.9 cm

R_2: RADIUS OF CORE ZONE 2 51.2 cm

D: THICKNESS OF RADIAL BLANKET 28.0 cm

FIG. 1 CONFIGURATION AND DIMENSIONS OF SNEAK ASSEMBLY 3A-1

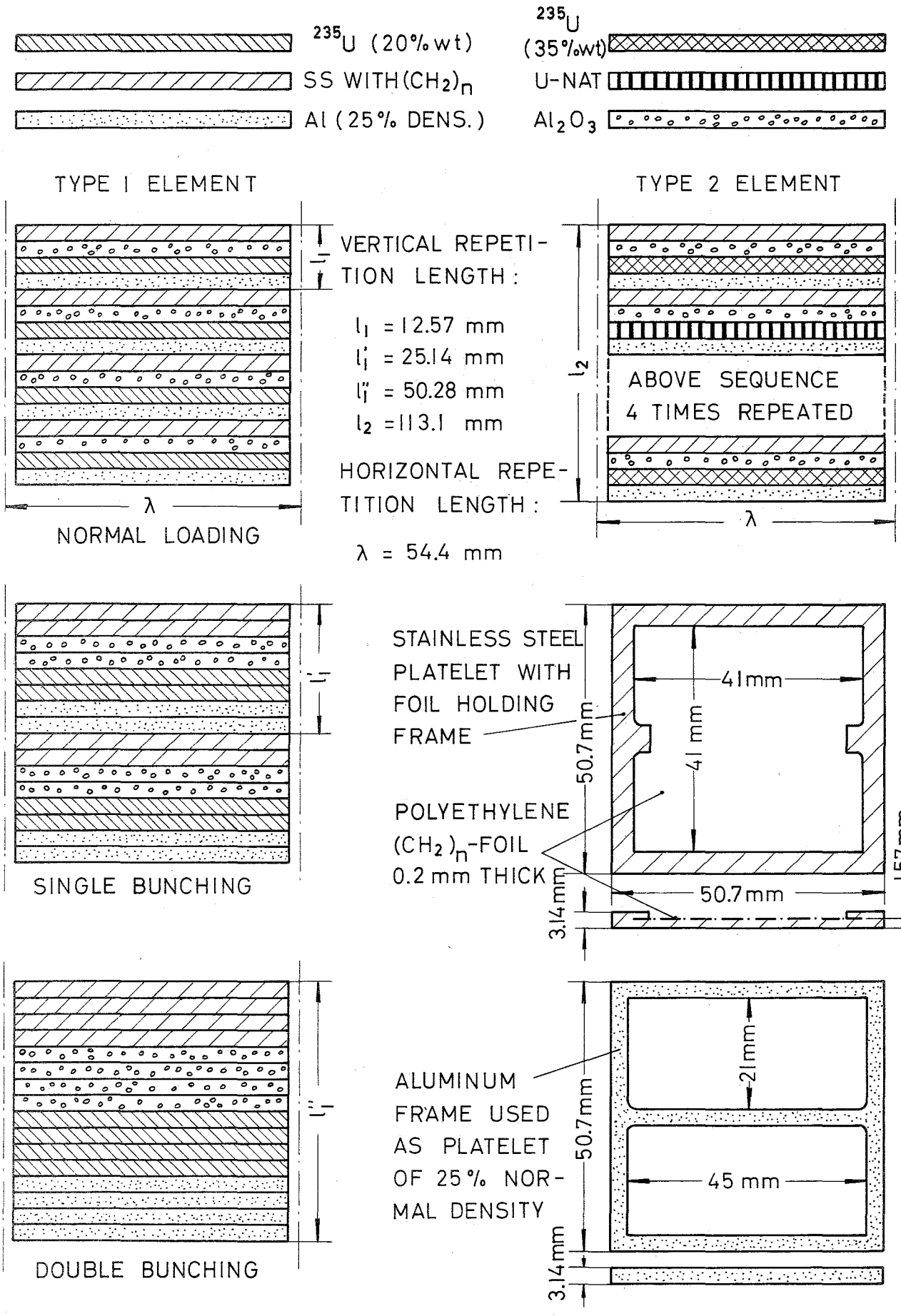

FIG. 2 CELL STRUCTURES AND SPECIAL PLATELETS USED IN SNEAK ASSEMBLY 3A-1

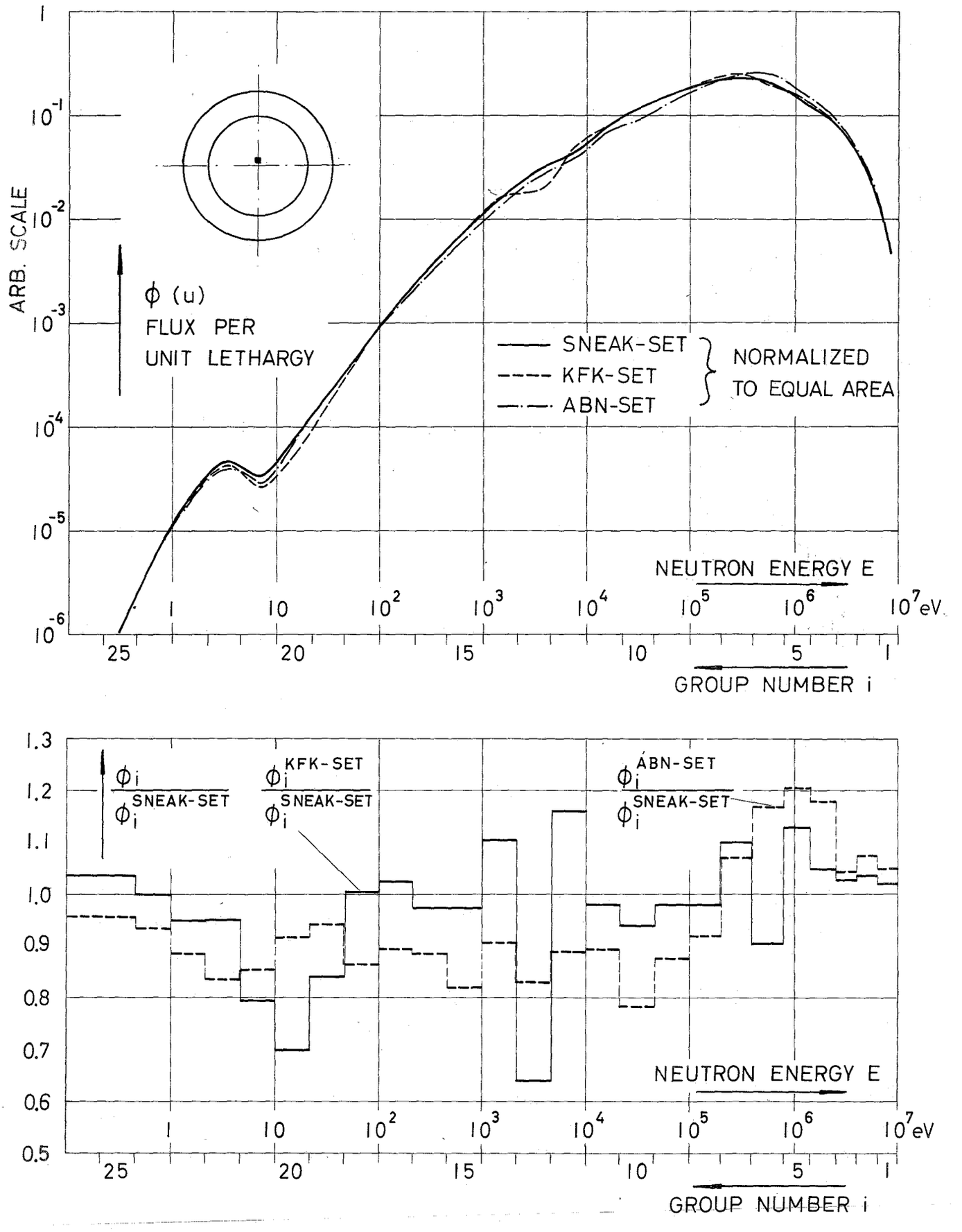

FIG. 3 COMPARISON OF CALCULATED NEUTRON SPECTRA AT THE CENTER OF 3A-1 USING DIFFERENT CROSS SECTION SETS

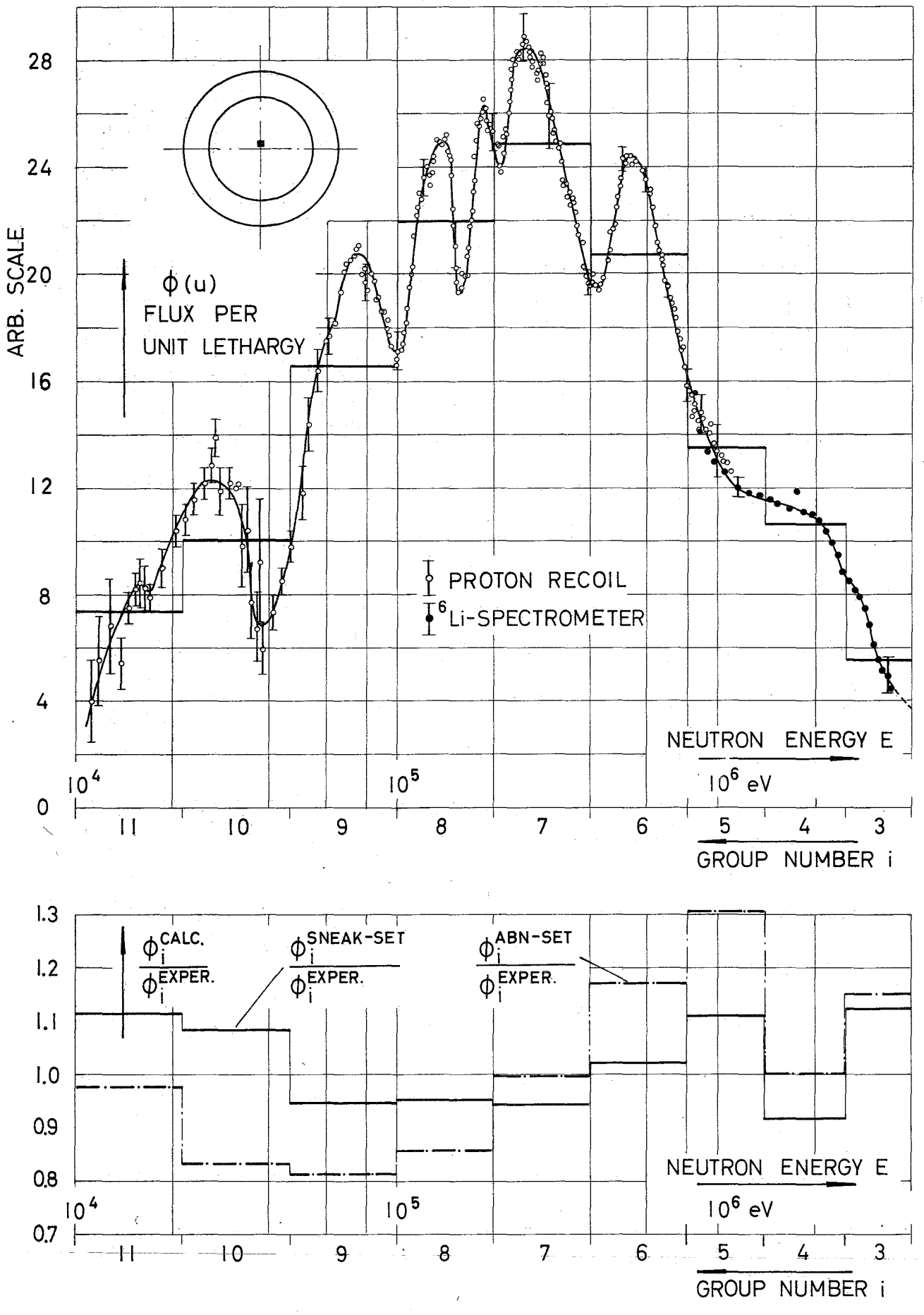

FIG. 4 COMPARISON BETWEEN CALCULATED AND MEASURED NEUTRON SPECTRUM AT THE CORE CENTER OF 3A-I

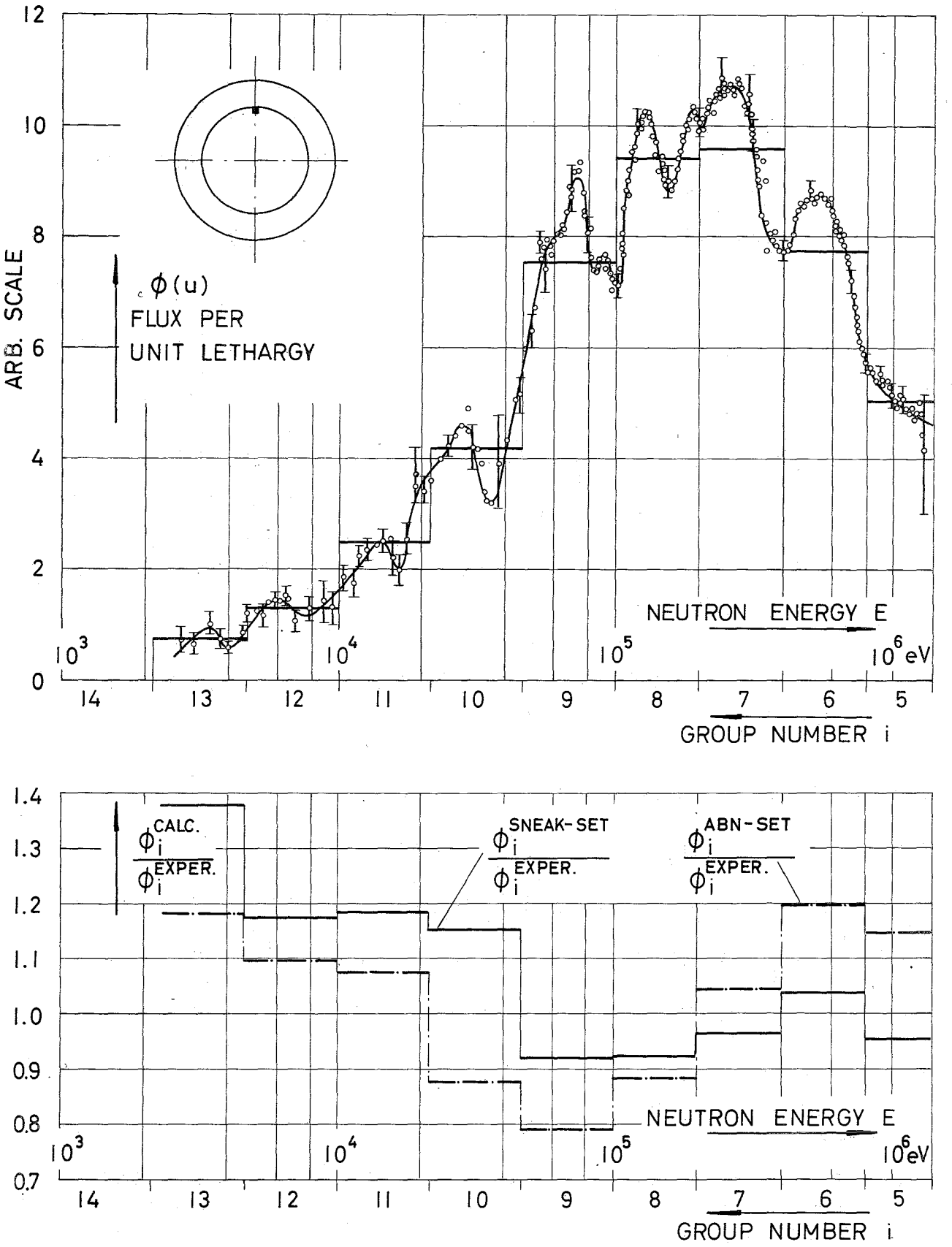

FIG. 5 COMPARISON BETWEEN CALCULATED AND MEASURED NEUTRON SPECTRUM AT THE CORE BOUNDARY OF 3A-1

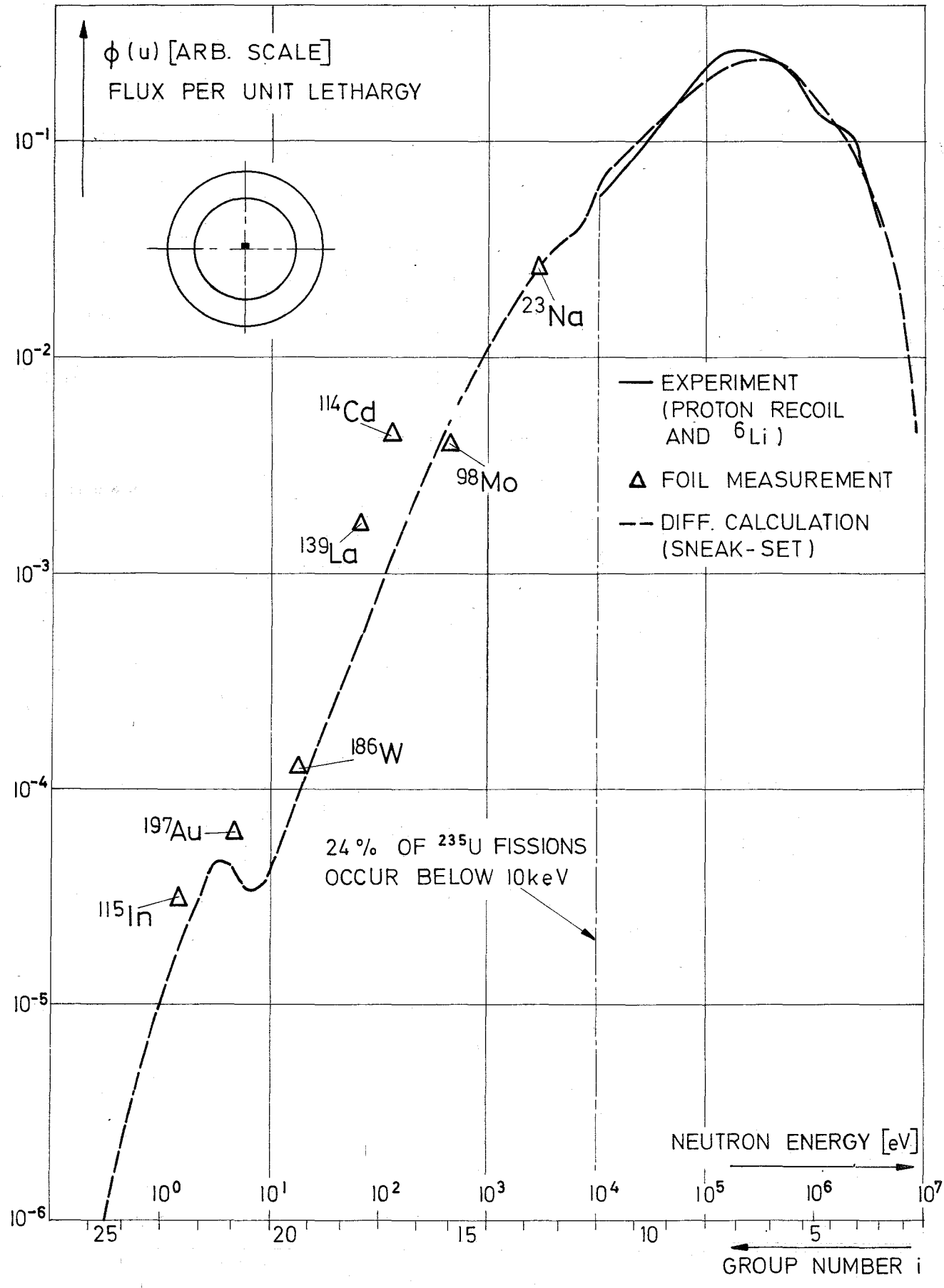

FIG.6 INVESTIGATION OF THE LOW ENERGY PART OF NEUTRON SPECTRUM AT THE CENTER OF 3 A - I

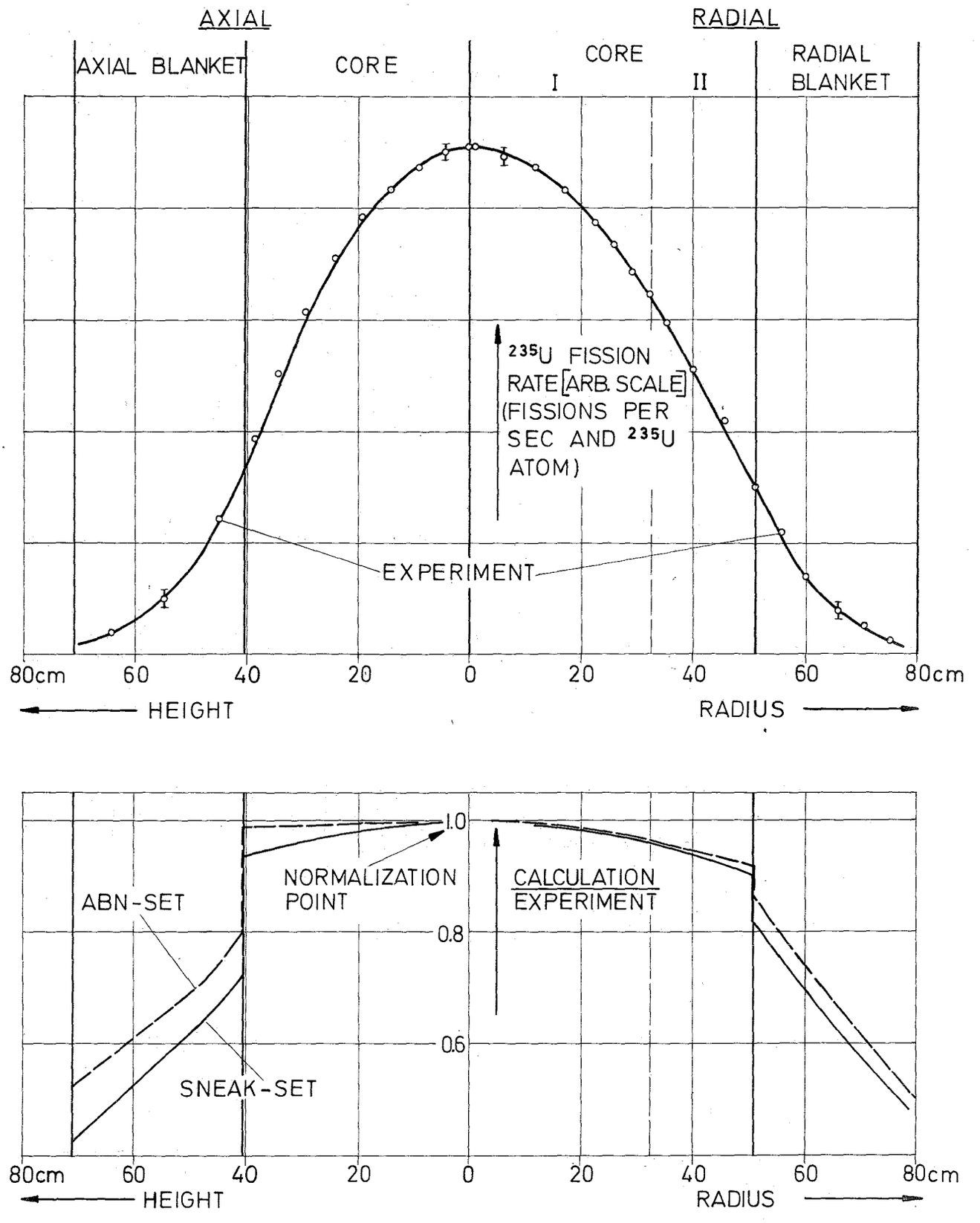

FIG. 7 COMPARISON OF MEASURED AND CALCULATED ^{235}U FISSION RATES IN SNEAK ASSEMBLY 3A-1

U-238 FISSION RATE TRAVERSES

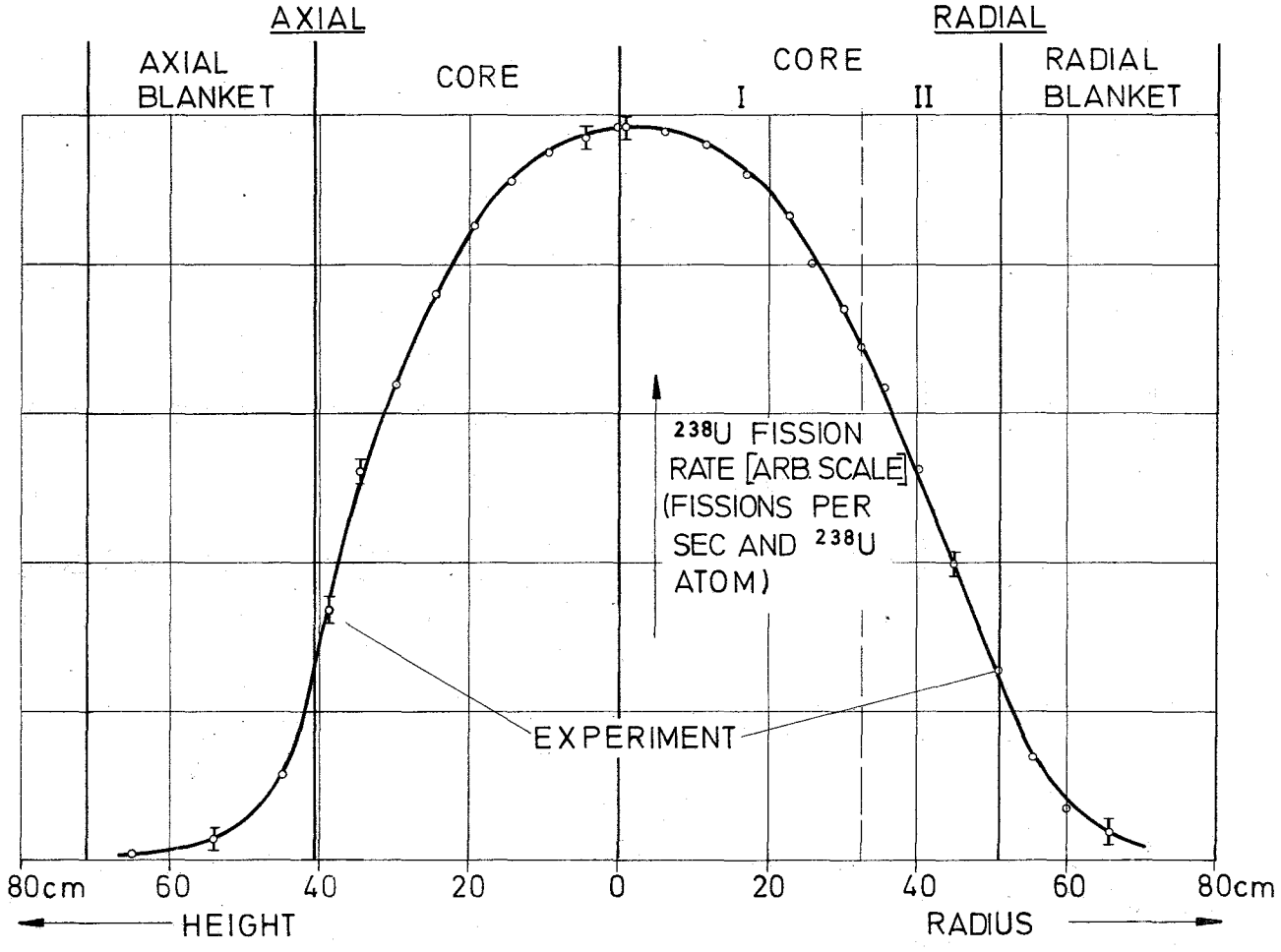

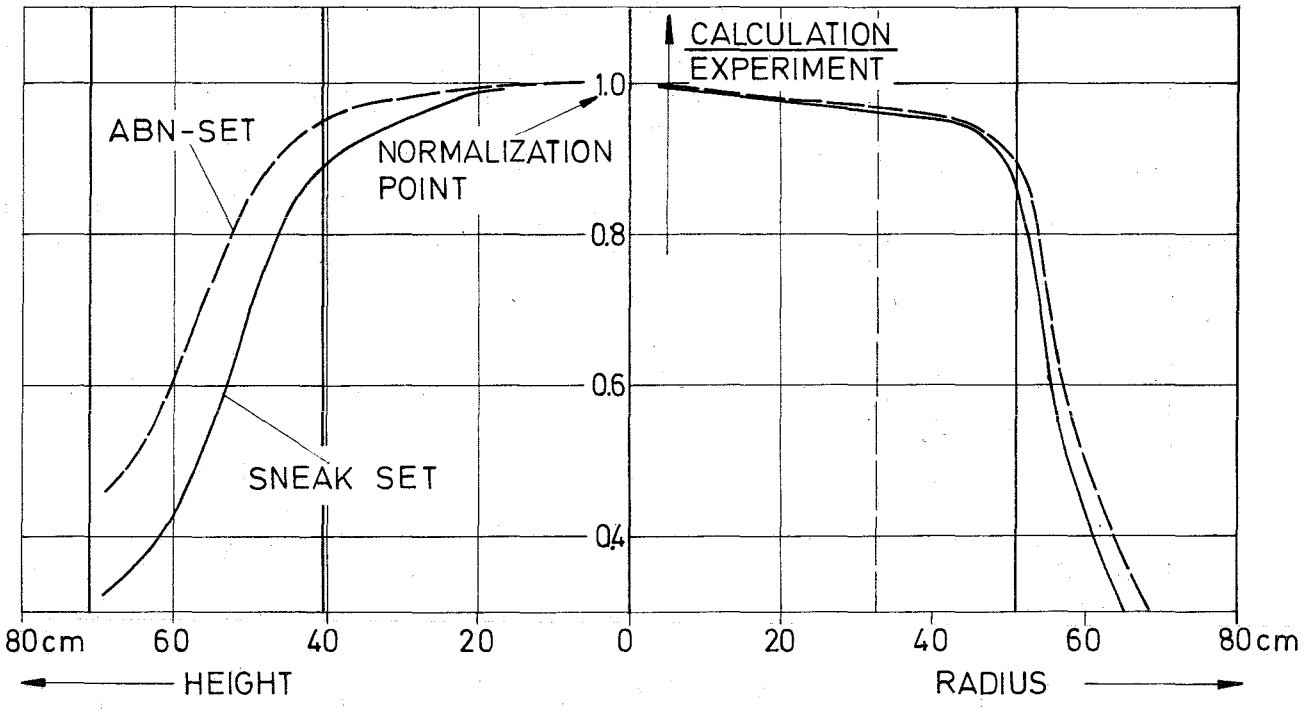

FIG. 8 COMPARISON OF MEASURED AND CALCULATED ^{238}U FISSION RATES IN SNEAK ASSEMBLY 3A-1

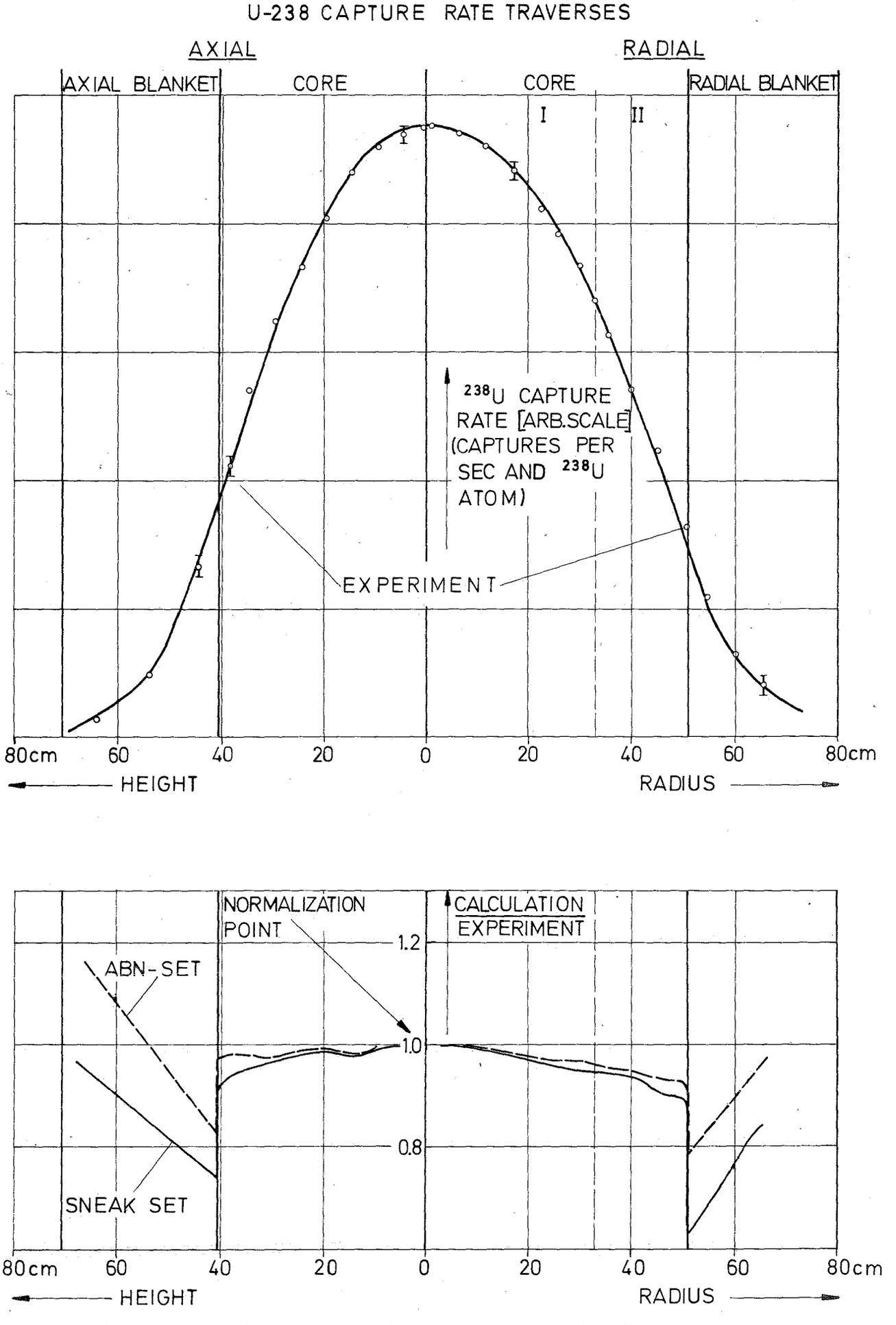

FIG. 9 COMPARISON OF MEASURED AND CALCULATED ^{238}U CAPTURE RATES IN SNEAK ASSEMBLY 3A-1

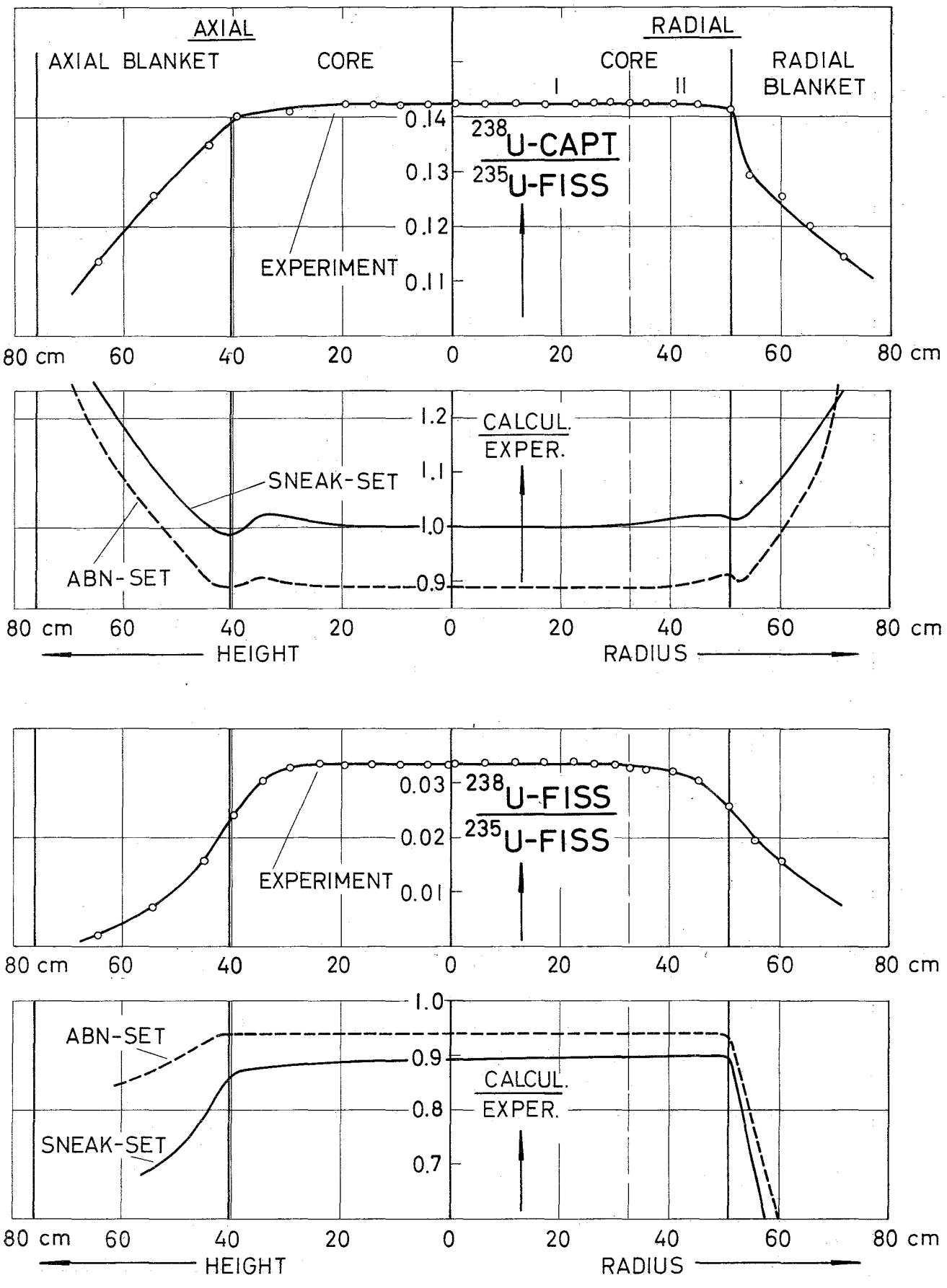

FIG. 10 COMPARISON OF MEASURED AND CALCULATED REACTION RATE RATIOS IN SNEAK ASSEMBLY 3A-1

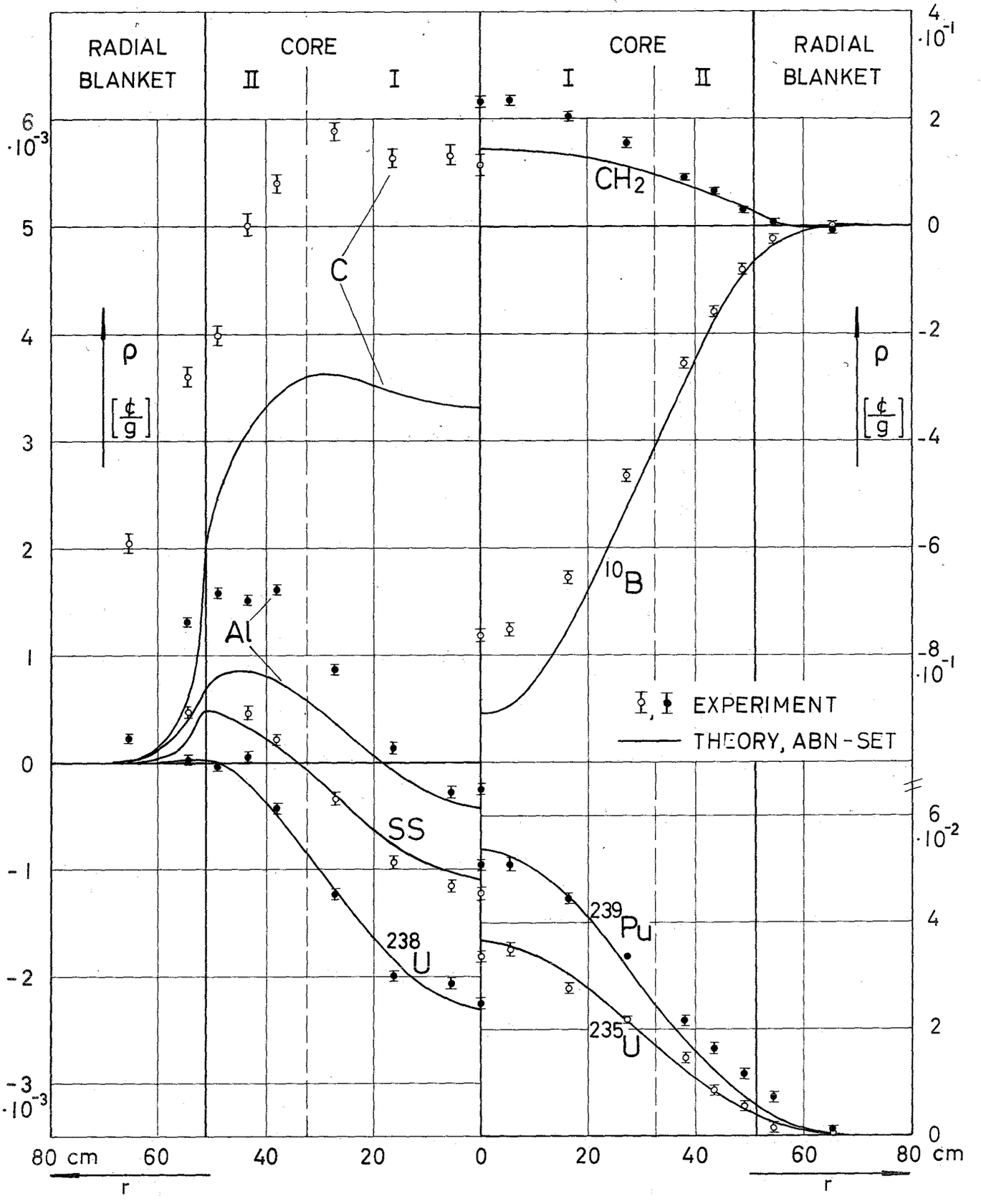

FIG. 11 RADIAL REACTIVITY TRAVERSES OF DIFFERENT MATERIALS IN SNEAK ASSEMBLY 3A-1

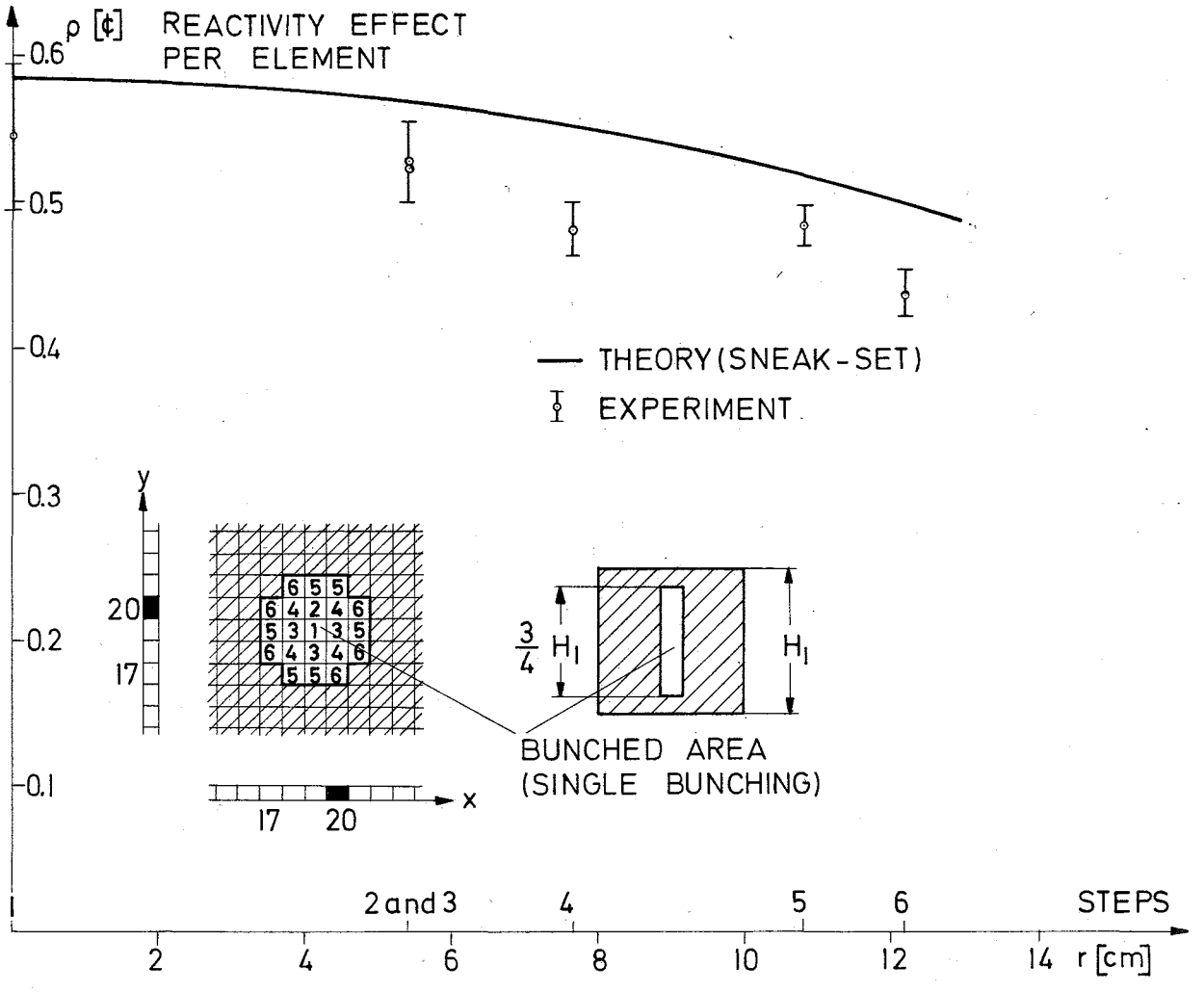

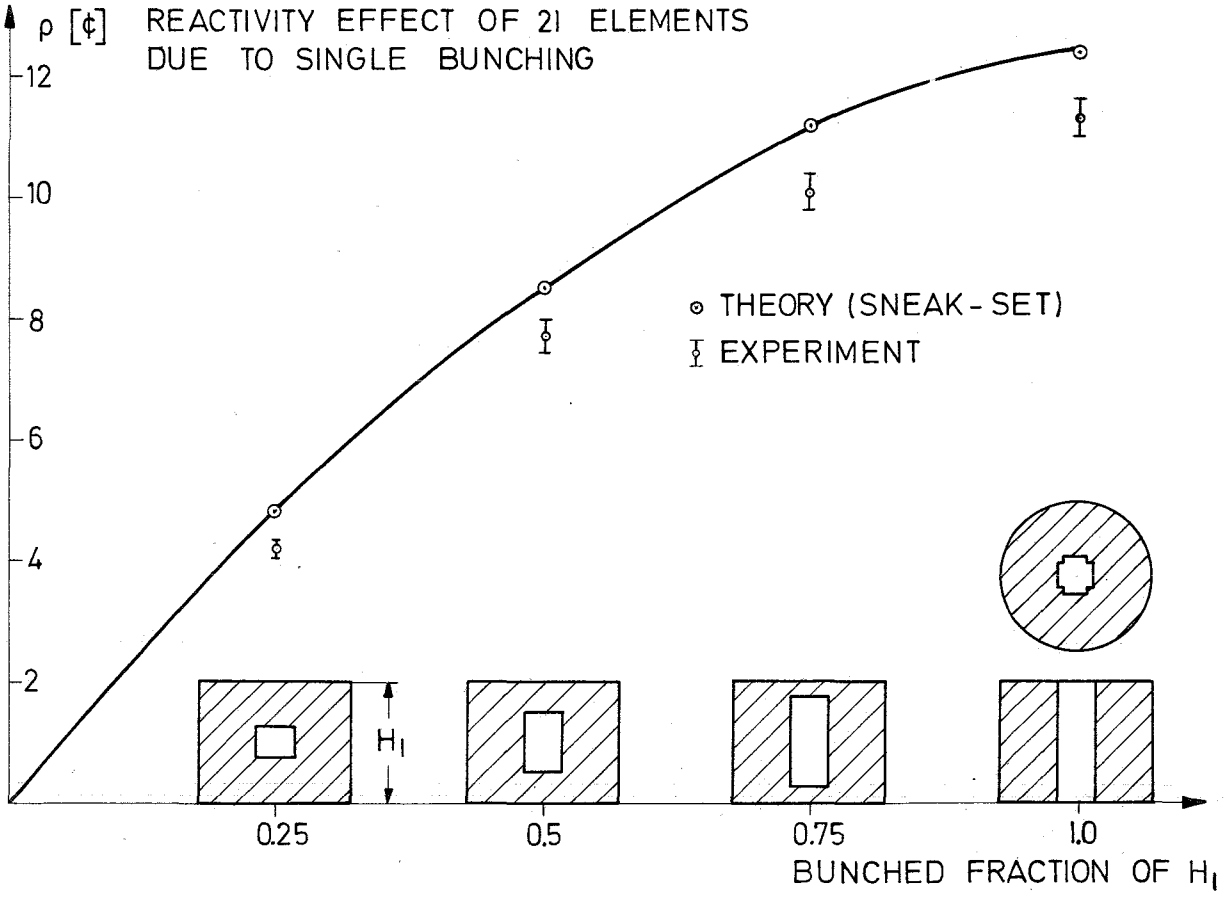

FIG.12 a,b RADIAL AND AXIAL REACTIVITY EFFECTS OF SINGLE BUNCHING IN SNEAK ASSEMBLY 3A-1

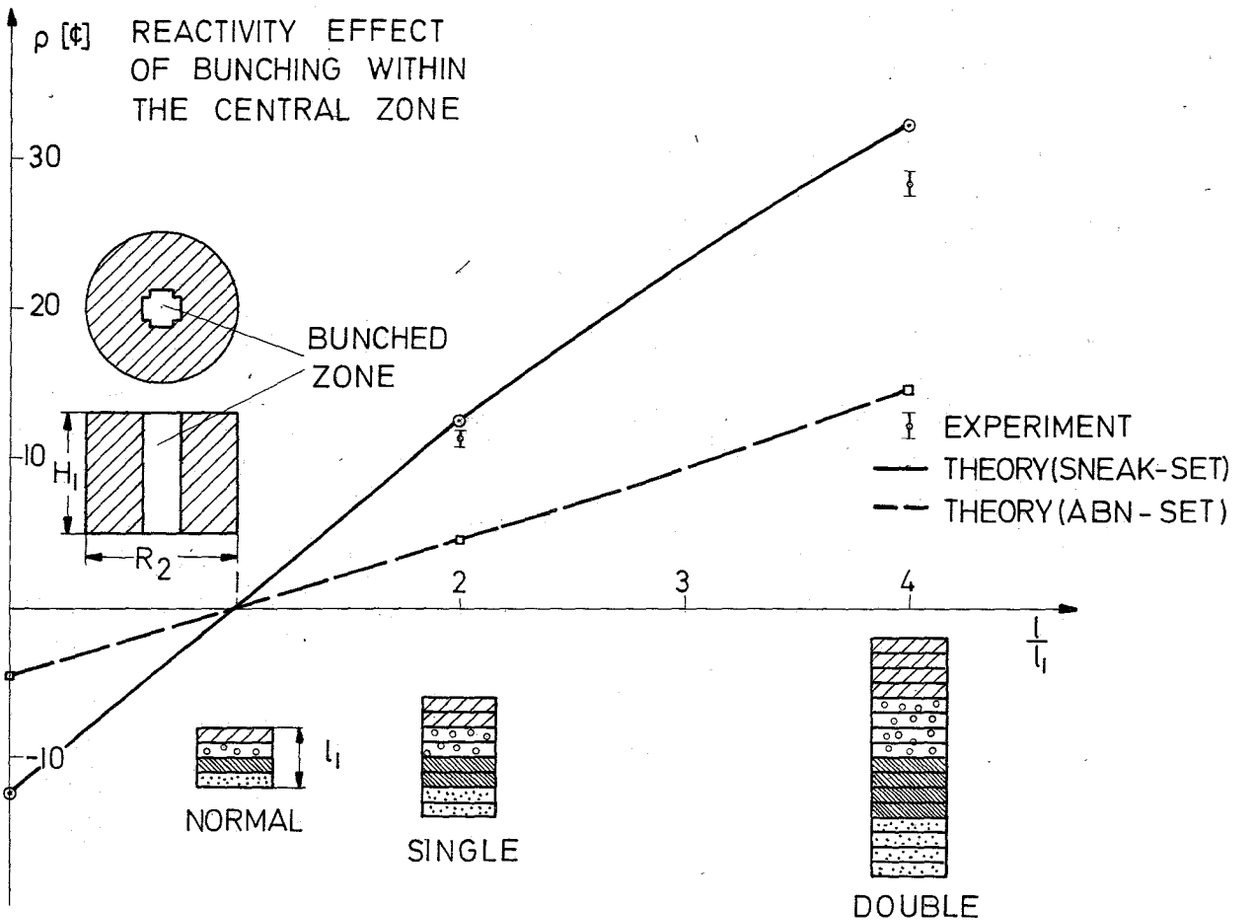

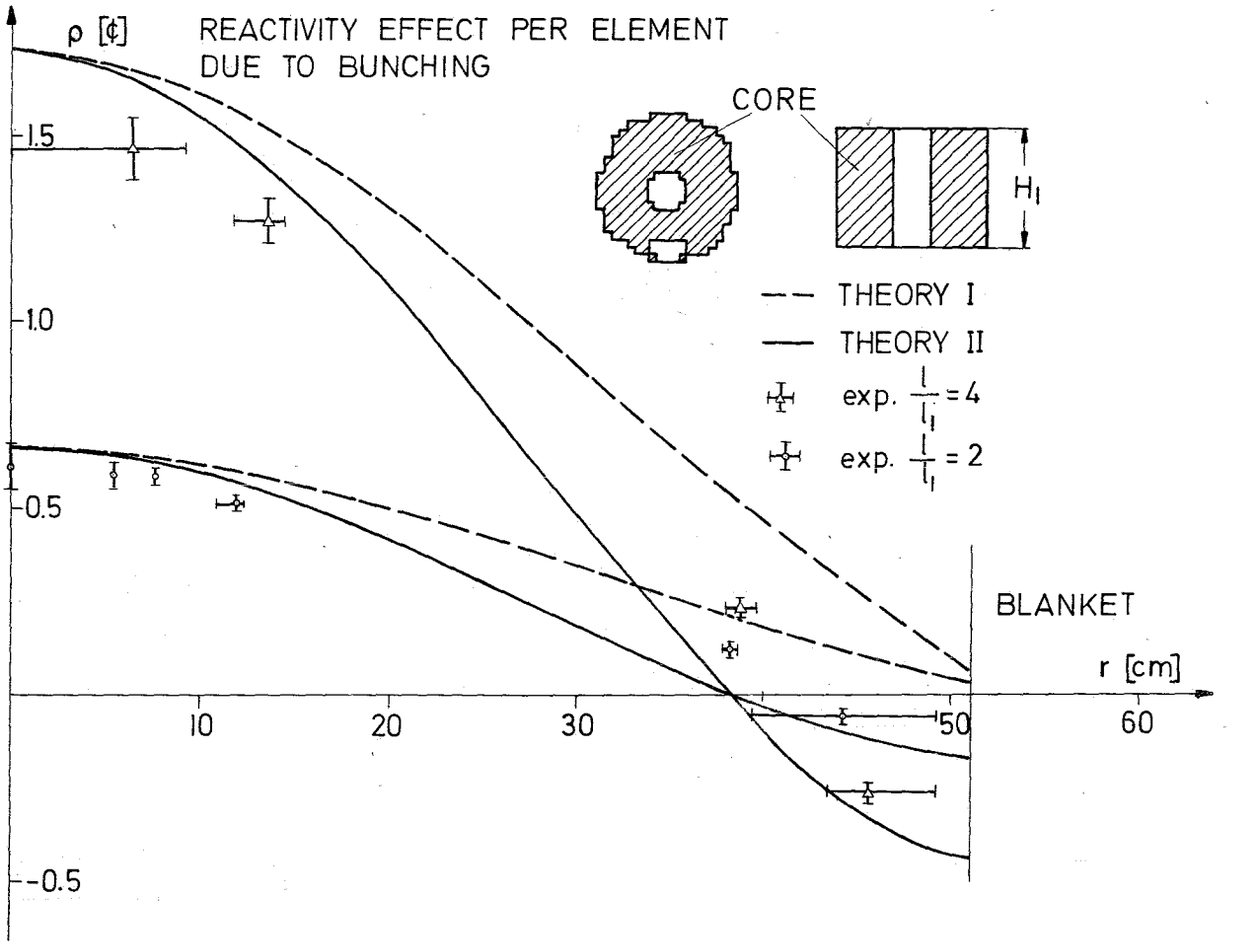

FIG. 13 a, b REACTIVITY EFFECTS OF SINGLE AND DOUBLE BUNCHING IN SNEAK ASSEMBLY 3A-1

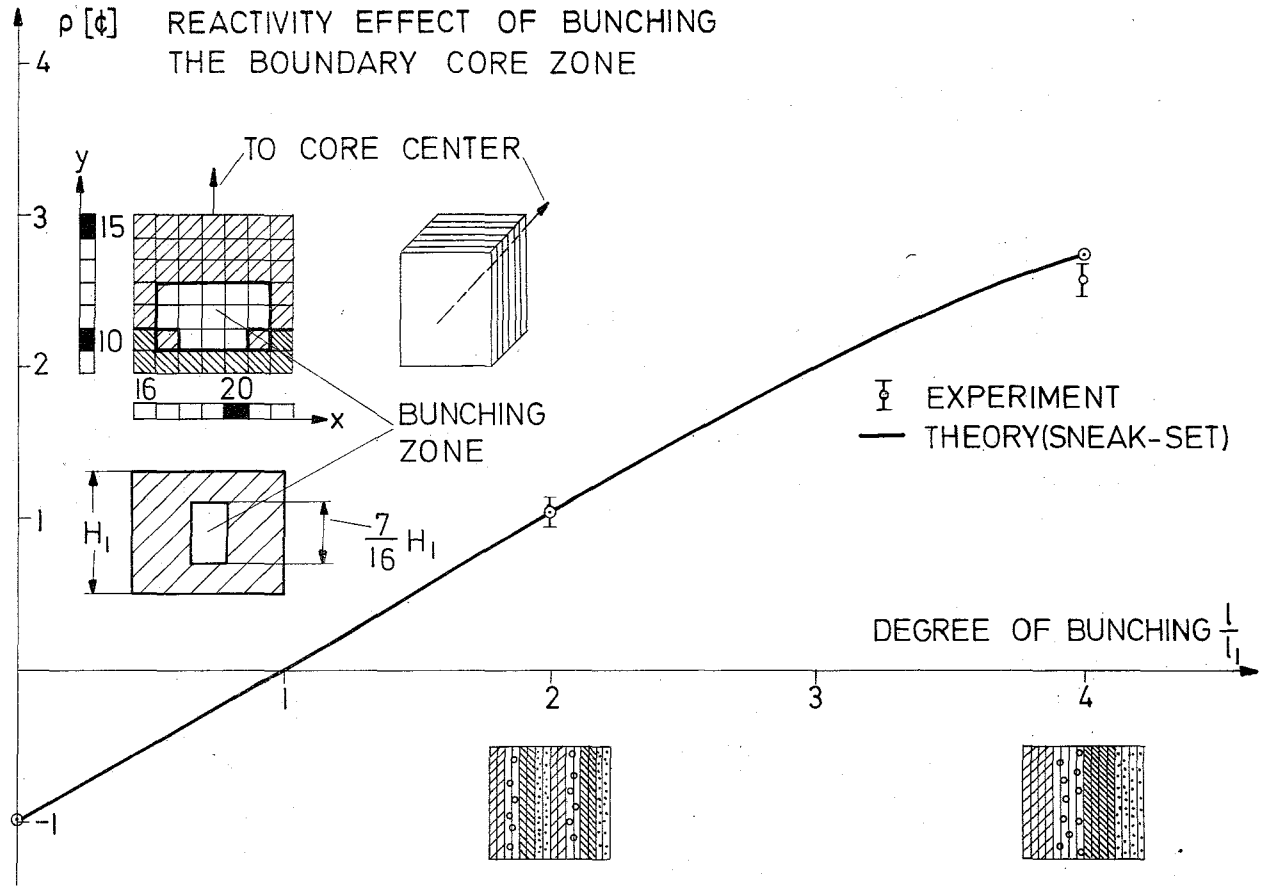

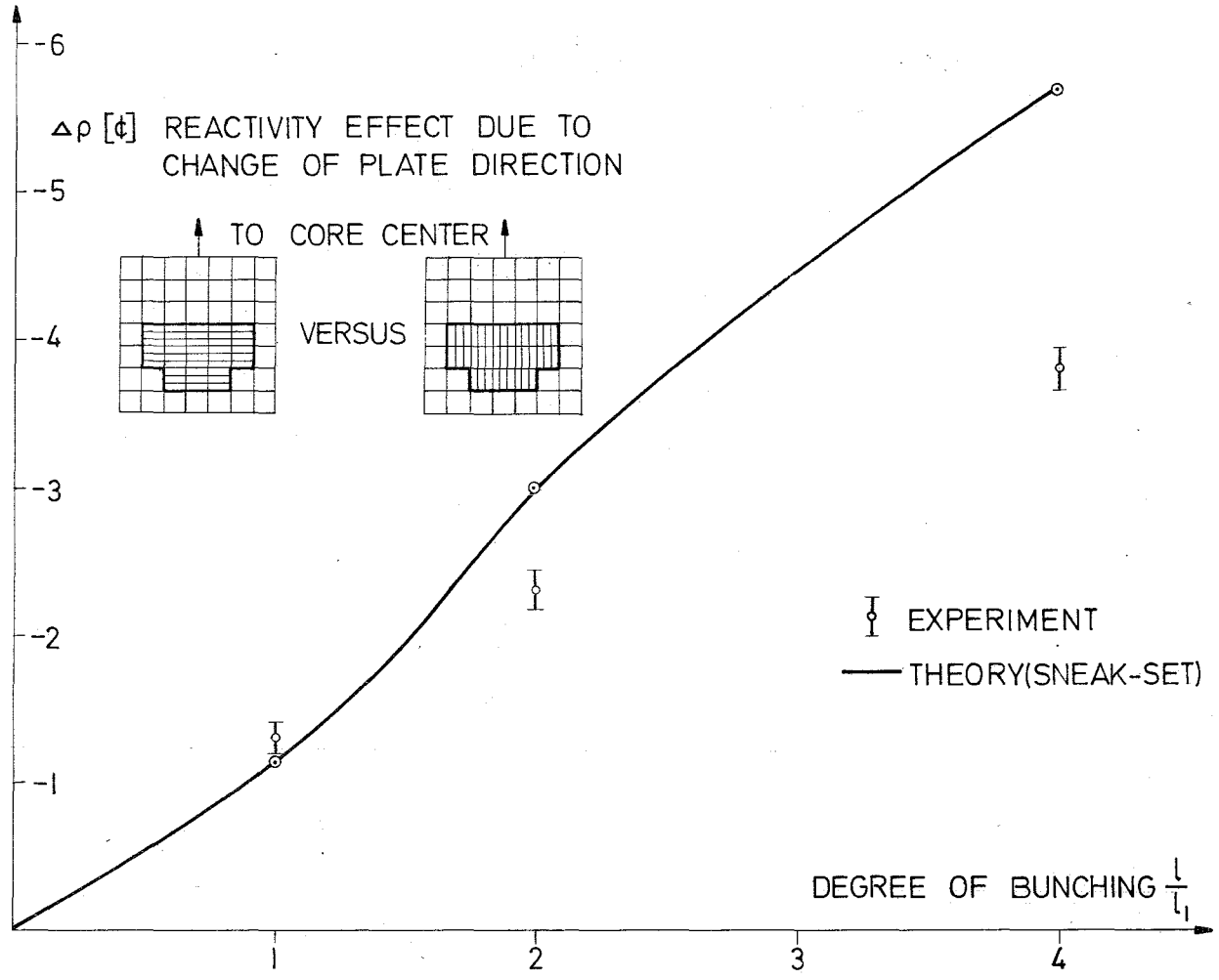

FIG.14 a,b REACTIVITY EFFECTS IN THE BOUNDARY CORE ZONE OF SNEAK ASSEMBLY 3A-1

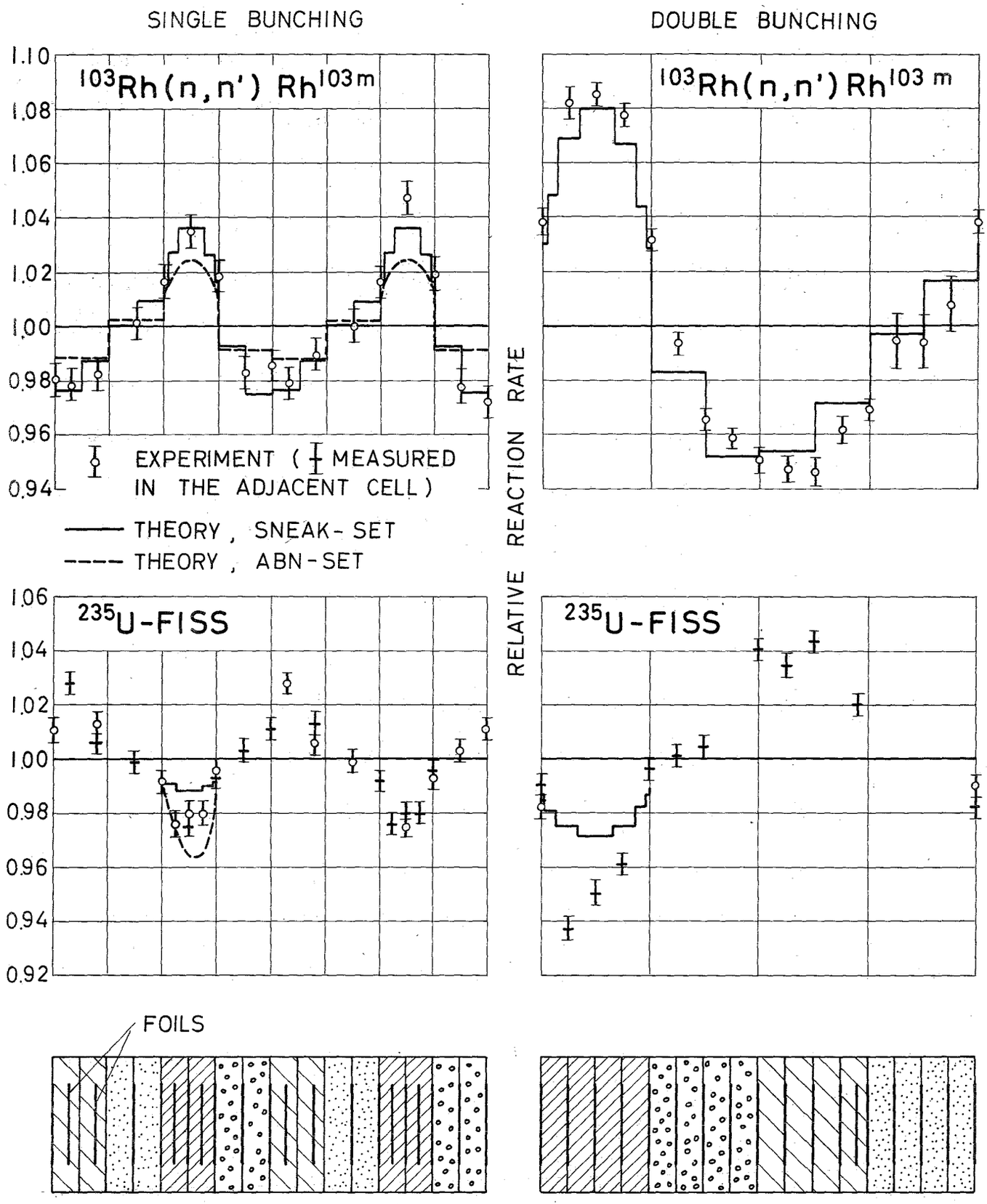

FIG. 15 FINE STRUCTURE AT THE CENTER OF SNEAK ASSEMBLY 3A-1

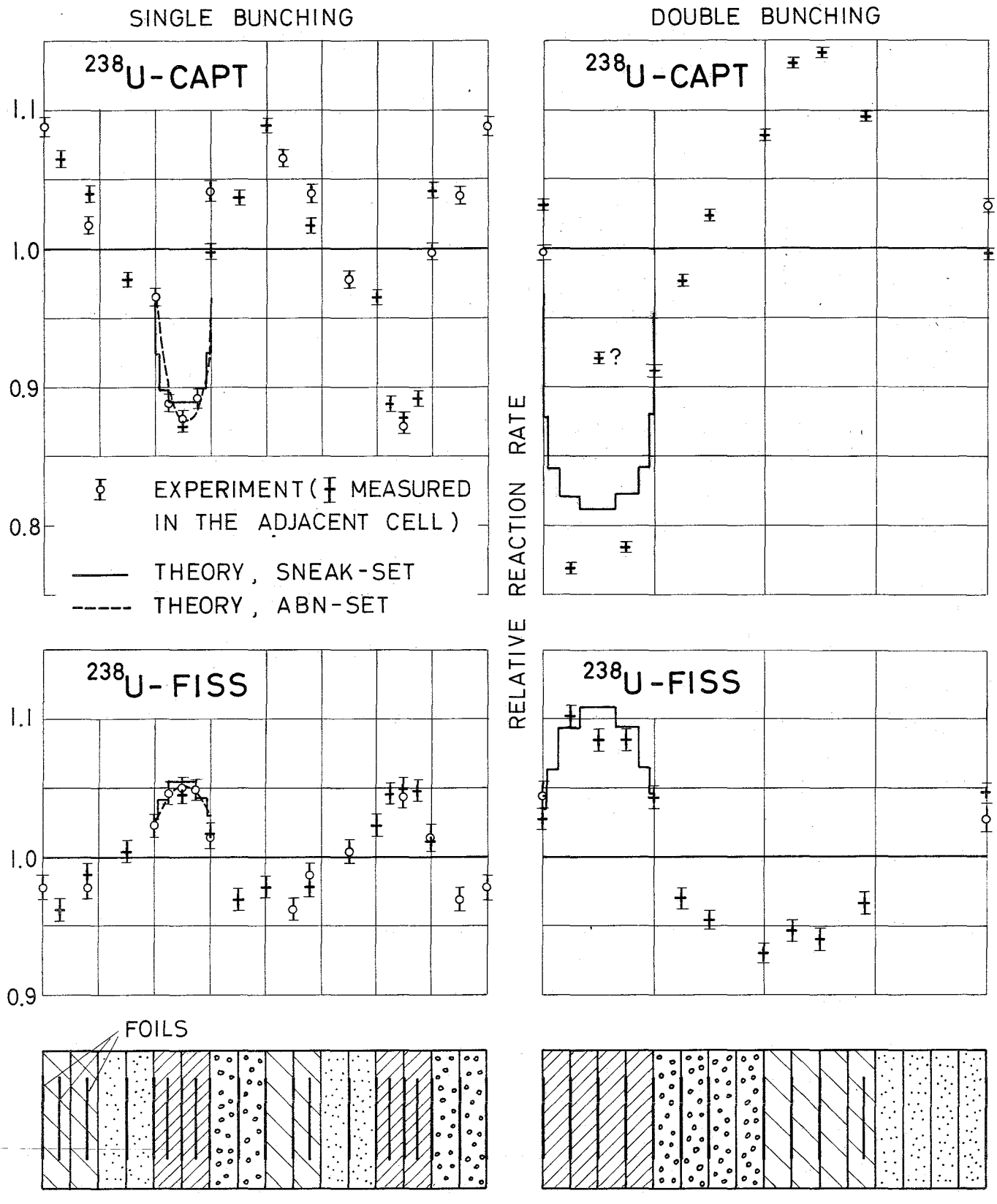

FIG. 16 FINE STRUCTURE AT THE CENTER OF SNEAK ASSEMBLY 3A-1

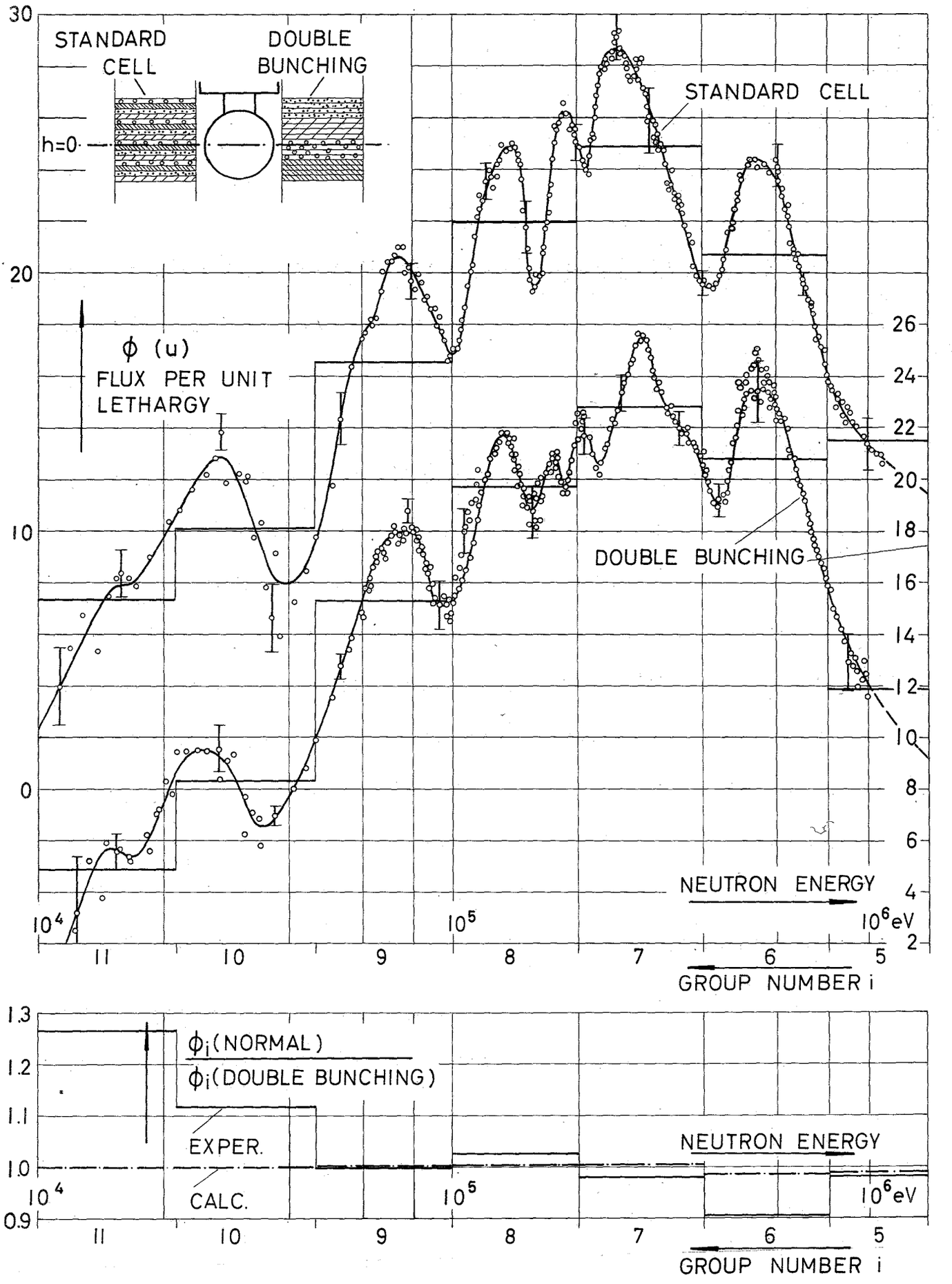

FIG. 17 COMPARISON BETWEEN NEUTRON SPECTRA OBTAINED WITH NORMAL AND DOUBLY BUNCHED CELL STRUCTURE IN SNEAK ASSEMBLY 3A-1

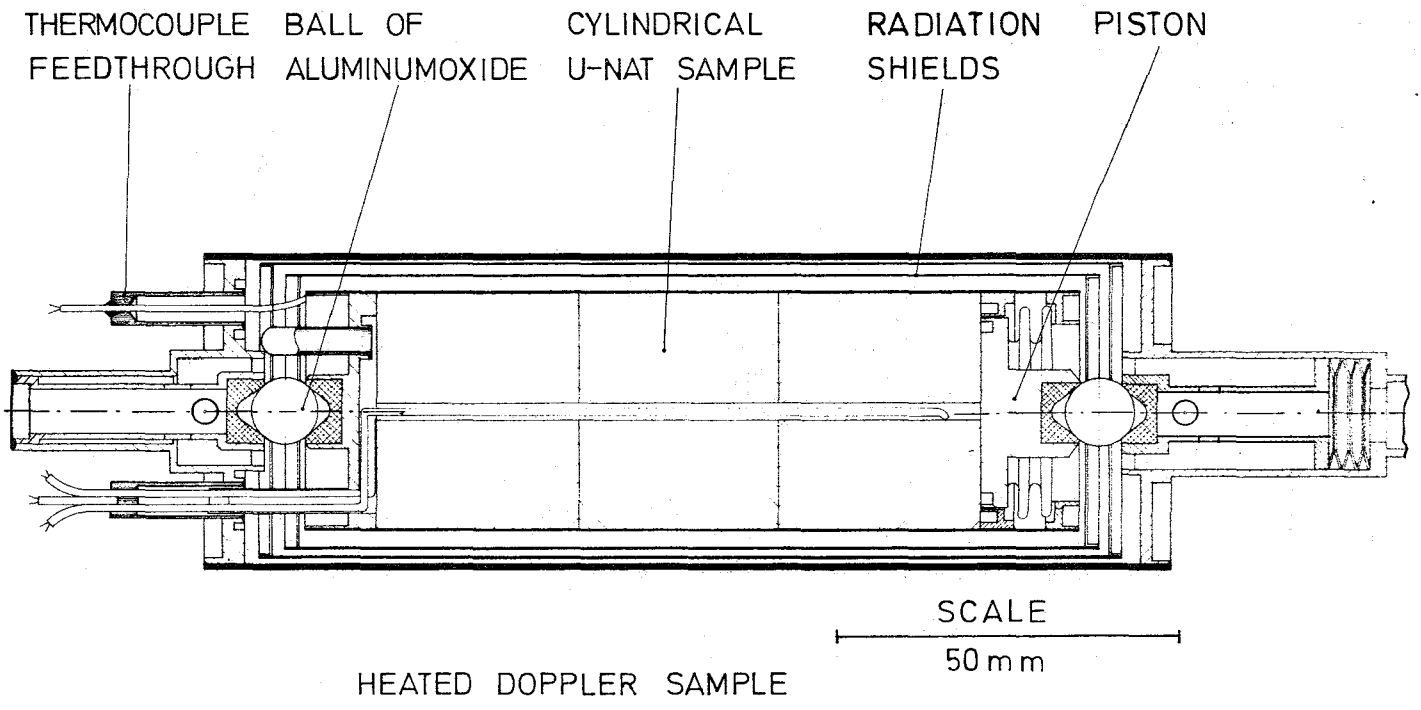

HEATED DOPPLER SAMPLE

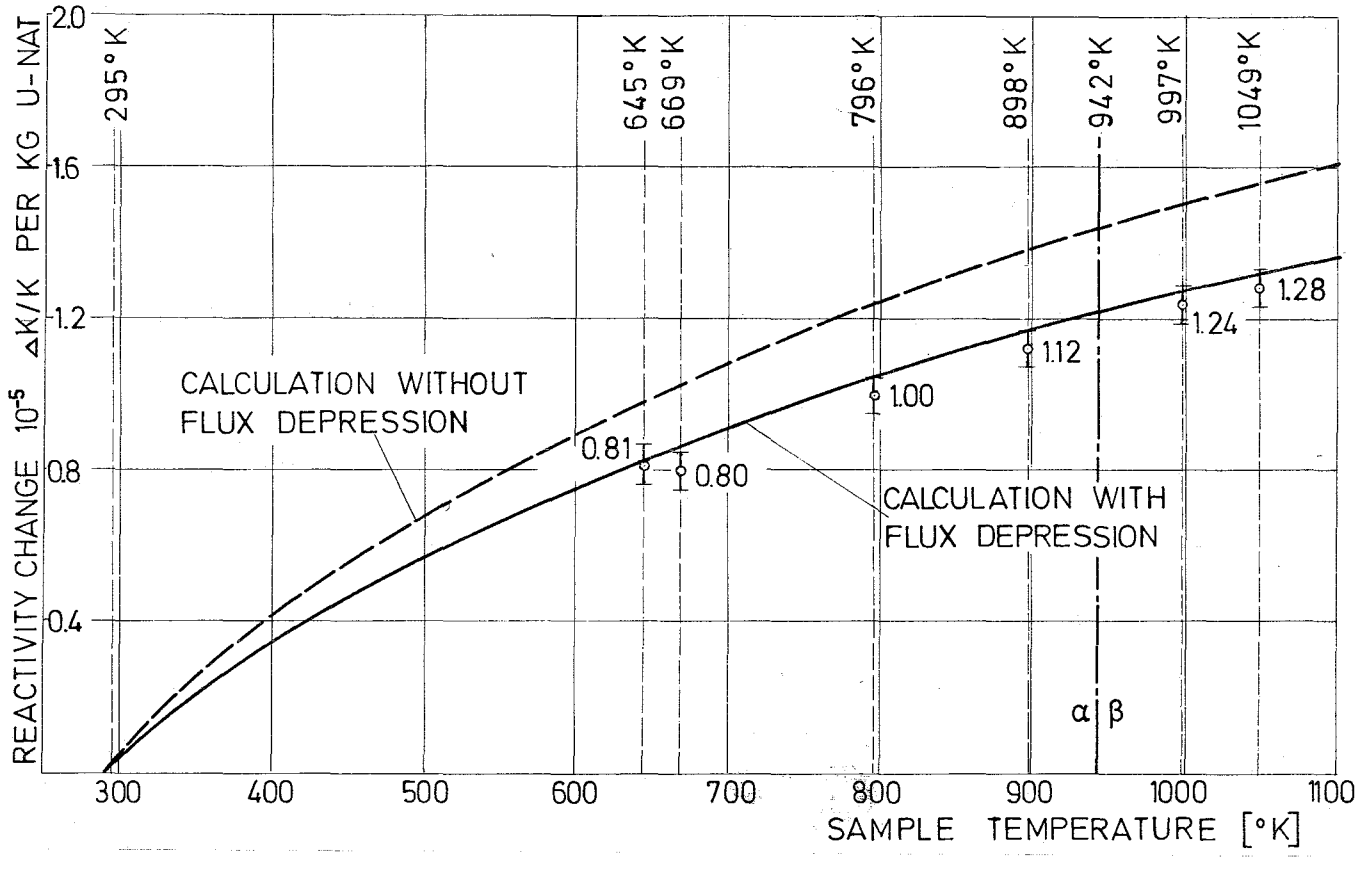

FIG.18 TEMPERATURE DEPENDENT REACTIVITY EFFECT OF METALLIC U-NAT DOPPLER SAMPLE IN ASSEMBLY 3A-1

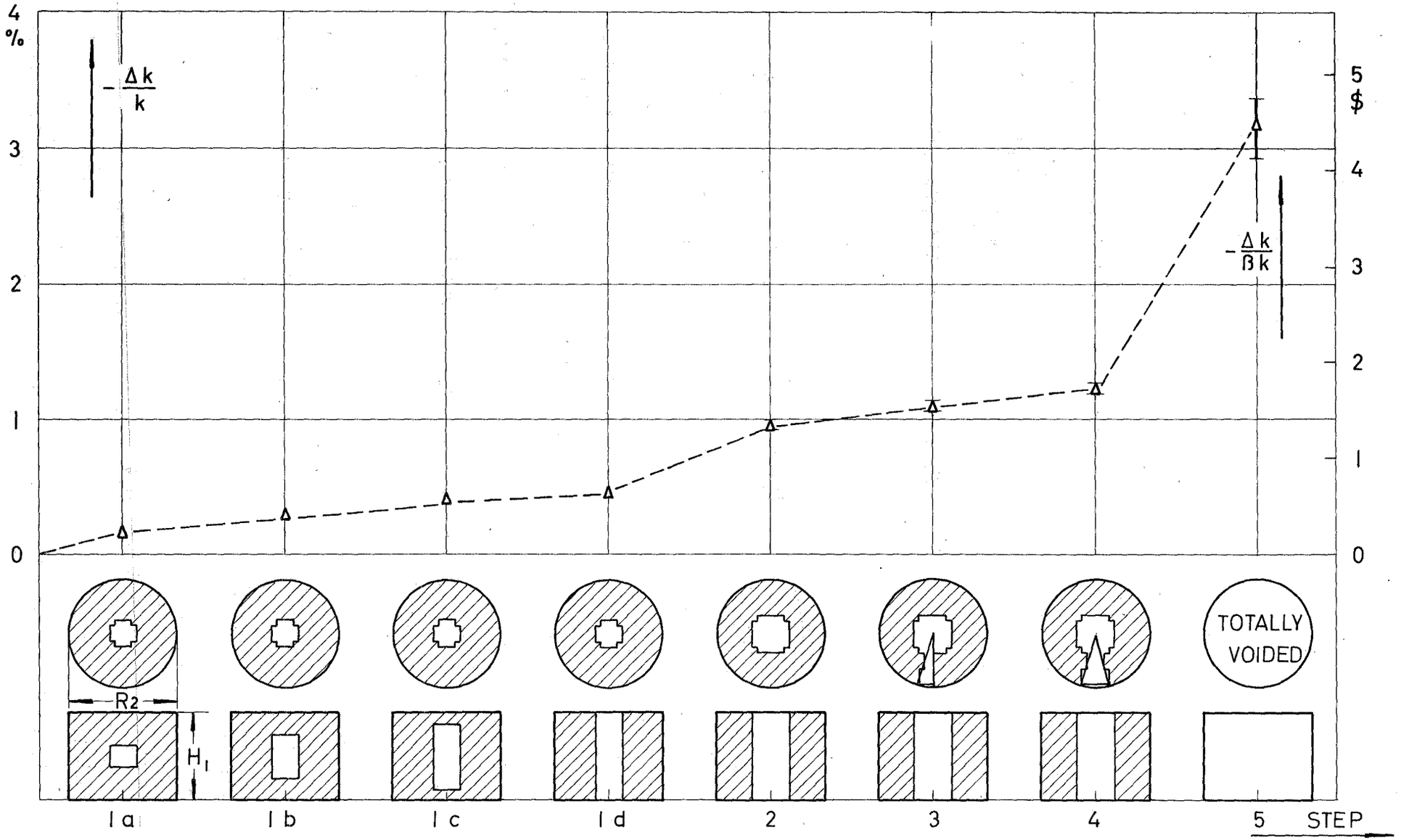

FIG. 19 MEASURED STEAM VOID EFFECT IN SNEAK ASSEMBLY 3A-1